Stability of dissolved and soluble Fe(II) in shelf sediment pore waters and release to an oxic water column

Klar, J.K.[a,b*], Homoky, W.B.[c], Statham, P.J.[a], Birchill, A.J.[d], Harris, E.L.[a], Woodward, E.M.S.[e], Silburn, B.[f], Cooper, M.J.[a], James, R.H.[a], Connelly, D.P.[g], Chever, F.[a], Lichtschlag, A.[g], Graves, C.[a]

[a] Ocean and Earth Science, University of Southampton, National Oceanography Centre, Southampton, SO14 3ZH, United Kingdom.
[b] Present address: LEGOS, Université de Toulouse, CNES, CNRS, IRD, UPS, 14 Avenue Edouard Belin, 31400 Toulouse, France.
[c] University of Oxford, Department of Earth Sciences, South Parks Road, Oxford, OX1 3AN, United Kingdom.
[d] School of Geography, Earth and Environmental Science, University of Plymouth, Drake Circus, Plymouth PL4 8AA, United Kingdom.
[e] Plymouth Marine Laboratory, Prospect Place, The Hoe, Plymouth, PL1 3DH, United Kingdom.
[f] Centre for Environment, Fisheries and Aquaculture Science, Pakefield Road, Lowestoft, NR33 0HT, United Kingdom.
[g] National Oceanography Centre, University of Southampton Waterfront Campus, European Way, Southampton, SO14 3ZH, United Kingdom.
[*]Corresponding author, email jessica.klar@legos.obs-mip

Keywords: Benthic iron flux, shelf sediment, oxic shelf, porewaters, iron isotopes, redox speciation, seasonality, ligands

Abstract

Shelf sediments underlying temperate and oxic waters of the Celtic Sea (NW European Shelf) were found to have shallow oxygen penetrations depths from late spring to late summer (2.2 to 5.8 mm below seafloor) with the shallowest during/after the spring-bloom (mid-April to mid-May) when the organic carbon content was highest. Sediment porewater dissolved iron (dFe, < 0.15 µm) mainly (> 85 %) consisted of reduced Fe(II) and gradually increased from 0.4 to 15 µM at the sediment surface to ~100 to 170 µM at about 6 cm depth. During the late spring this Fe(II) was found to be mainly present as soluble Fe(II) (> 85 % sFe, < 0.02 µm). Sub-surface dFe(II) maxima were enriched in light isotopes (δ^{56}Fe of -2.0 to -1.5 ‰), which is attributed to dissimilatory iron reduction (DIR) during the bacterial

decomposition of organic matter. As porewater Fe(II) was oxidised to insoluble Fe(III) in the surface sediment layer, residual Fe(II) was further enriched in lighter isotopes (down to -3.0 ‰). Ferrozine-reactive Fe(II) was found in surface porewaters and in overlying core top waters, and was highest in the late spring period. Shipboard experiments showed that depletion of bottom water oxygen in late spring can lead to a substantial release of Fe(II). Reoxygenation of bottom water caused this Fe(II) to be rapidly lost from solution, but residual dFe(II) and dFe(III) remained (12 and 33 nM) after > 7 hours. Iron(II) oxidation experiments in core top and bottom waters also showed removal from solution but at rates up to 5-times slower than predicted from theoretical reaction kinetics. These data imply the presence of ligands capable of complexing Fe(II) and supressing oxidation rates. The lower oxidation rate allows more time for the diffusion of Fe(II) from the sediments into the overlying water column. Modelling indicates significant diffusive fluxes of Fe(II) (on the order of 23-31 µmol m^{-2} d^{-1}) are possible during late spring when oxygen penetration depths are shallow, and pore water Fe(II) concentrations are highest. In the water column this stabilised Fe(II) will gradually be oxidised and become part of the dFe(III) pool. Thus oxic continental shelves can supply dFe to the water column, which is enhanced during a small period of the year after phytoplankton bloom events when organic matter is transferred to the seafloor. This input is based on conservative assumptions for solute exchange (diffusion-reaction), whereas (bio)physical advection and resuspension events are likely to accelerate these solute exchanges in shelf-seas.

Introduction

Whilst iron (Fe) is a major constituent of the solid Earth, dissolved Fe (dFe) concentrations in oxic waters are very low (typically < 1 nM) because of the limited solubility of oxidised forms of the metal. However, this element and its redox cycling have major impacts on the cycling of other elements (e.g., P) in terrestrial waters and during diagenesis in sediments (Raiswell and Canfield 2012). Iron is also an essential micro-nutrient for marine primary producers and is a limiting factor in ~25 % of the open ocean (Boyd and Ellwood 2010), due to its low availability. As marine primary productivity plays a significant role in CO_2 uptake from the atmosphere, Fe is argued to be important in the regulation of the global climate (Sigman

and Boyle 2000). It is therefore important to understand how Fe is supplied to the ocean from different sources, and how it is cycled and removed. Typically, Fe concentrations are highest close to sources (atmospheric inputs, hydrothermal vents, rivers and the seafloor). For shallow shelf and slope waters, rivers are anticipated to be only a small source because of extensive removal of Fe in low salinity waters during estuarine mixing (Sholkovitz et al. 1978). Atmospheric inputs are most significant where dust inputs are large, and are directly delivered to the photic zone (de Jong et al. 2007). However, sediments underlying shelf and slope waters are argued to be a major source of Fe that can ultimately be transferred to the ocean (Johnson et al. 1999; Elrod et al. 2004; Severmann et al. 2010; Homoky et al. 2012; Conway and John 2014; Dale et al. 2015).

Within marine sediments, dissimilatory iron reduction (DIR) by bacteria can produce large inventories of soluble Fe(II) in ferruginous zones of interstitial porewaters during the decomposition of organic matter (Burdige 2006). These Fe(II) maxima carry diagnostically light isotopic signals, typically -2.0 to -1.0 ‰ (Severmann et al. 2006; Homoky et al. 2009; Severmann et al. 2010). It is widely accepted that towards the oxic sediment-water boundary Fe(II) is oxidised to Fe(III), and lost to insoluble Fe(III) oxides. This oxidative trap prevents transfer of most of the sediment sourced dFe to oxic seawater. This process is associated with the removal of heavy Fe isotopes leading to further enrichment of light Fe isotopes in the porewater (Severmann et al. 2006; Homoky et al. 2009). Within more oxidizing sediments, the isotopic signature of dFe is close to crustal compositions, e.g., 0.0 to 0.2 ‰ (Homoky et al. 2009; 2013), and the dFe fraction consists mainly of Fe colloids (0.02-0.2 µm), that are argued to originate from “non-reductive” dissolution processes (Radic et al. 2011; Homoky et al. 2011; 2013). The Fe isotopic composition in the water column may serve as a tool to trace benthic Fe fluxes which originate from different dissolution processes and are transported to the ocean interior (Conway and John 2014).

The processes involved in the supply of Fe from sediments to shelf seas, and its fate in the water column, are not yet fully understood. Benthic chamber measurements have shown that the largest fluxes of dFe are released from continental margin sediments with high inventories of organic carbon and reactive iron minerals underlying oxygen-depleted waters (Severmann et al. 2010; Dale et al. 2015). However, few studies have examined the

92 Fe cycle in oxic shelf seas, even though they represent a large fraction of the ocean's
93 continental boundaries (Homoky et al. 2016). There are many reports of oxic shelf waters
94 with higher dissolved Fe (dFe) than the open ocean (Charette et al. 2007; Cullen et al. 2009;
95 de Jong et al. 2012; Marsay et al. 2014) and hence they may also be a significant source to
96 the ocean in the global Fe cycle.

97 The mechanisms involved in the supply of Fe from sediments to the overlying water
98 include diffusion of Fe from porewaters, sediment resuspension by bottom boundary
99 currents, or tidal currents and bio-turbation and bio-irrigation. Whilst a geochemical
100 overview exists for the cycling of Fe in marine sediments (e.g., Burdige 2006) details of
101 processes that can lead to transfer of dFe to oxic shelf seas are lacking. From a seasonal
102 perspective in temperate systems, large amounts of organic matter of bloom origin are
103 deposited onto the seafloor during spring. The organic matter gradually decomposes,
104 leading to the release of remineralised nutrients and Fe into porewaters and across the
105 sediment-water interface. However, to date there are no data that document the seasonal
106 changes in porewater Fe in such systems, or the controls on dFe exchange between
107 sediments and the water column. It is crucial to obtain estimates of Fe fluxes from different
108 types of shelf environments to better constrain global supply rates in biogeochemical
109 models that feed into global climate models (Homoky et al. 2016).

110 This study is part of an extensive research programme in the Celtic Sea (Thompson et
111 al. submitted). The Celtic Sea is a temperate, shallow (< 200 m) and oxic shelf sea, which
112 undergoes deep mixing during winter and becomes more stratified in summer (Williams et
113 al. 2013; Thompson et al. submitted). The shelf system has a broad connection to the
114 adjacent North Atlantic Ocean, and provides an ideal setting to study processes controlling
115 the sedimentary dissolution and release of Fe to the overlying water column. Here we
116 present a seasonal study of Fe cycling within cohesive sediments of the Celtic Sea shelf,
117 examining the form and fate of Fe in porewaters, and mechanisms whereby this Fe may be
118 released to overlying waters.

Materials and Methods

Sampling of sediments, porewaters and seawater

All laboratory apparatus, filters and sample bottles used for low concentration Fe determinations were cleaned using a rigorous acid washing regime, including different dilutions of HCl (up to 2 M) and ultrapure purified water (Milli-Q, resistivity of 18.2 MΩ·cm).

Sediments were collected from cohesive Site A (sandy mud ~51˚ 12.6754' N, 6˚ 8.0277' W) and Site I (muddy sand ~ 50° 34.5557 N, 7° 6.3161 W) within the Celtic Sea. Sediments from these sites distinguish themselves in mean grain size and porosity (for more details, see Thompson et al. submitted). This study mainly focuses on Site A sediments, while a couple of experiments were run with sediments from Site I. Sediments were collected using pre-drilled clear polycarbonate core tubes (60 cm length, 10 cm diameter) mounted on a Bowers and Connelly Mega Corer, which grants minimal sediment disturbance during collection. The Celtic Sea was revisited twice during 2015, on the RRS *Discovery* cruises DY030 (4th to 25th May, 2015, late spring conditions) and DY034 (6th August to 2nd September, 2015, late summer conditions). The spring bloom started in early April, had fully developed bloom conditions on the 19th of April and lasted until mid-May. Therefore, DY030 captures part of the end of the bloom and post-bloom conditions and DY034 occurred 2 - 3 months after the bloom. On each visit undisturbed sediment cores with clear overlying water were selected and taken into a temperature-controlled laboratory (set to bottom water temperature) on the vessel. Excess core top water was siphoned through Teflon and Tygon tubes into a low-density polyethelyene (LDPE) bottle, and immediately filtered through 0.2 µm filters (Cyclopore, Whatman) in a Nalgene filtration unit. Each filtrate was sub-sampled for dFe, dFe isotope and nutrients into LDPE bottles. After core top water sampling, oxygen depth profiles were measured by microsensors (see below) and the residual core top water was siphoned to waste.

With core top water removed, porewaters were extracted from sediments cores at 1 to 2 cm depth intervals using Rhizon samplers (Seeberg-Elverfeldt et al. 2005). The MOM-type Rhizon samplers (Rhizosphere Research Products B.V., 50 mm long, 2.5 mm diameter, 0.15 µm pore size) were inserted at right angles through PVC tape that covered the pre-

drilled holes in the core tube walls, and attached via luer-lock fittings to nitrile-free syringes (20 ml, BD Discardit). At each depth, suction was applied and then, after discarding the first 0.5 ml to waste, a porewater sample was collected. This approach allows for the fast extraction and handling of porewater samples (Homoky et al. 2013), and effectively isolates redox sensitive trace metals from oxidation artefacts. Subsample aliquots were immediately fixed with the synthetic Fe(II) ligand ferrozine (3-(2-pyridyl)-5,6-diphenyl-1,2,4-triazine) for ship-board Fe(II) and total Fe analyses (details below). Porewater subsamples for dFe isotopes and dMn were stored in clean LDPE bottles and acidified to pH 1.8 with distilled concentrated HCl. Subsamples for nutrients were taken for ship-board analysis. During cruise DY030, the soluble size fraction (< 0.02 µm, sFe) of porewaters was also collected through a nitrogen gas-purged Anotop25 syringe filter (Whatman), of which subsamples were immediately fixed with ferrozine for ship-board Fe(II) and total Fe analyses, and subsamples stored for sMn.

After porewater extraction, the residual sediment of one core from each season was sliced using a polycarbonate sheet at 0.5, 1 and 2 cm depth-intervals, and stored at -20° C in zip-lock bags prior to further analyses.

Water column samples were collected using a titanium rosette fitted with 24 x 10 L Ocean Test Equipment (OTE) water samplers adapted for trace metal work and coupled to a conductivity-temperature-depth (CTD) system (Seabird 911+), as well as oxygen, transmissiometer and fluorometer sensors (rosette hereafter called Ti-CTD). All sampling procedures followed GEOTRACES protocols as reported in the *Sampling and Sample-handling Protocols for GEOTRACES Cruises* (http://www.geotraces.org/).

Analytical methods

Analytical methods are described in detail in the Supplementary Information document. Oxygen profiles in sediment cores and O_2 monitoring in Fe(II) oxidation experiments were measured with Unisense O_2 micro sensors. The LOD was ≤ 0.3 µM.

The concentrations of Fe species - Fe(II) and Fe(II) plus Fe(III) (hereafter total Fe) – were determined in the dissolved and soluble size fractions of porewater samples using the Fe(II)-complexing ferrozine ligand (Sigma-Aldrich) (Stookey 1970; Viollier et al. 2000).

Concentrations > 1 µM Fe(II) were measured on a spectrophotometer (ATI Unicam 8625) and concentrations < 1 µM Fe(II) were measured on a 250 cm 3000 Series Liquid Waveguide Capillary Cell (LWCC, World Precision Instruments) (Waterbury et al. 1997). On the spectrophotometer, the limit of detection (LOD, three times the standard deviation of the blank) was 0.3 µM Fe(II) and the blank was 0.25 µM Fe(II). The typical relative standard deviation (obtained by measuring replicates) was 2 % for > 10 µM and up to 5 % below 4 µM. For the LWCC, the LOD was 0.7 nM, the blank was 6 ± 4 nM and the typical relative standard deviation was < 5 %.

The concentration of dFe(II) in the water column was determined using flow injection chemiluminescence using luminol (Bowie et al. 2002; Ussher et al. 2007). The LOD of this method (defined as three times the standard deviation of the blank) was 15 pM Fe(II) and the blank was 25 pM Fe(II). The average relative standard deviation, obtained from triplicate analyses, for all samples above the LOD was 6.7 %.

A $^{57}Fe/^{58}Fe$ double spike technique was used to determine the isotopic composition of Fe in porewaters, seawater samples and core-top waters (Lacan et al. 2010; Conway et al. 2013). Samples were analysed on a Neptune *Plus* (Thermo Scientific) with an external reproducibility of ±0.04 ‰ (2 SD).

Porewater Mn concentrations in soluble and dissolved size fractions were determined in diluted samples on a quadrupole ICP-MS (X-Series, Thermo Scientific). The blank was < 0.8 nM, the LOD was 0.2 nM and the typical relative standard deviation was 2 %.

In order to examine phase associations of Fe and Mn in solid sediment phases, two leaching schemes were applied to one core per season: (i) an ascorbic acid leach (Raiswell et al. 2010) was applied, to extracts the easily reducible oxide phases, such as amorphous ferrihydrite, but not the more crystalline oxide phases, and (ii) an acetic acid-hydroxylamine-HCl (H-HCl) leach (Berger et al. 2008), to extract other amorphous oxide phases as well as ferrihydrite. Fe and Mn in the leach solutions were determined using an inductively coupled plasma optical emission spectrometer (ICP-OES, iCAP6000 Series, Thermo Scientific). For Fe, the blank was < 0.06 µg/g, the LOD was < 4 µg/g and the typical standard deviation was ~20

206 µg/g. For Mn, the blank was < 0.02 µg/g, the LOD was < 0.6 µg/g and the typical standard
207 deviation was 4 µg/g.

208 Nutrient concentrations in water column samples, in sediment porewaters and
209 experiments, were all analysed on board using a Bran and Luebbe segmented flow
210 colorimetric auto-analyser (Woodward and Rees 2001). The typical relative standard
211 deviation was 2-3 %; and the LODs were 0.02, 0.01, and 0.05 µmoles L^{-1} for "nitrate plus
212 nitrite", nitrite, and ammonia, respectively. Sulphide was measured using the colorimetric
213 technique of Cline (1969), and the detection limit was 1 µM.

214 Particulate organic carbon (POC) and nitrogen (PON) were determined using a Carlo-
215 Erba CHNOS analyser (Nieuwenhuize et al. 1994). Precision was 6.6 % RSD at 1.5 % POC and
216 2.4 % RSD at 0.13 % PON. Estimated detection limit for C was 3.6 µg and all sample carbon
217 contents were well above this value.

218 ## Shipboard experiments

219 In order to study conditions that are potentially important for the transfer of dFe across the
220 sediment surface, a series of shipboard micro-cosm experiments were carried out on the
221 late spring and late summer cruises. Experiments were performed in the ship's constant
222 temperature laboratory set to ambient bottom water conditions, and used acid washed (> 1
223 M HCl) equipment and analytical procedures adapted for low concentration Fe analyses
224 described previously.

225 The first experiment was designed to assess the qualitative impact of periodic water
226 column deoxygenation on the diffusive release of dFe and dFe(II) from sediment cores to
227 overlying water, and further to see how rapidly Fe would be lost upon re-oxygenation of the
228 overlying water. The experiment was run on both, late spring and late summer sediment
229 cores and with water samples. One sediment core and its overlying bottom water was
230 sealed from the ambient atmosphere and the depletion of oxygen was induced – due to
231 microbial respiration within the experiment – for about a week in the dark. Then, the sealed
232 core was opened and aerated, while kept in the dark. During aeration the oxygen
233 concentration in overlying water was monitored continuously, and sub-samples of seawater

were used to assess dFe(II) and dFe at several time intervals during this re-oxidation processes over a period of ~2 days.

The second set of experiments was designed to measure the rates of dFe(II) oxidation in selected bottom waters in the presence and absence of sediments. The experiments were carried out in late summer only, on bottom waters collected with the titanium rosette ~10 m above the seafloor, and on bottom water overlying sediment cores (two replicates) collected at Site I (muddy sand). An Fe(II) standard (diluted from ammonium Fe(II) sulphate hexahydrate, Sigma Aldrich, purum p.a. grade) was added to these water samples for a target concentration of 200 nM Fe(II). The Fe(II) spiked waters were kept in the dark to ensure no photo-reduction of Fe(III) occurred, and the waters were sub-sampled (typically 15 times) over a period of ~4 hours to monitor the rates at which dFe(II) decreased over time.

The third experiment (carried out during late summer only) investigated any diffusive flux of dFe(II) and dFe across the sediment water interface, by periodically subsampling core top water overlying sediments, which were collected from Site I. For further details, see supplementary information.

Results

The shallowest and most variable oxygen penetration depths (OPDs) were observed in late-spring at our study site (Site A), coincident with the end of the spring bloom. OPDs ranged from 2.2 to 5.8 mm during the late spring (average 3.3 ± 1.1 mm, n = 11) and from 3.4 to 5.6 mm during late summer (average 4.1 ± 0.7 mm, n = 8; Figure 2). Based on replicate determinations of OPD, a t-test (0.07) strengthens our view that OPD was significantly (p <0.1) shoaled in late spring compared to late summer. We used a one-dimensional steady-state oxygen diffusion-consumption model to approximate the rates of organic C oxidation by fitting calculated outputs to the observed mean oxygen depth profile from each season. The reduction of squared residuals between modelled and observed values was used to optimize the model fit. The approach follows (Berner 1980), in which a single pool of reactive organic C is attributed to oxygen consumption and the influences of bioturbation,

seasonal sediment accumulation and porosity structure are ignored, as described elsewhere (e.g., Papadimitriou et al. 2004; Homoky et al. 2013). Oxygen consumption rates are found to be greatest in the late-spring, corresponding to a proportionally higher rate of organic carbon oxidation in the sediments (11.9 mmol m^{-2} d^{-1}) compared to the late summer season (8.6 mmol m^{-2} d^{-1}; Figure 2).

Porewater nitrate maxima were similar in late spring and late summer seasons, between 1 and 7 µM in the surface 0-1 cm (Figure 3). Porewater ammonia increases with depth in both seasons consistent with nitrate conversion to ammonia. Nitrate concentrations were higher in bottom waters (~ 8 µM; Figure 3), whereas ammonia concentrations were lower.

Porewater Mn concentrations had similar trends during both seasons, with shallow sub-surface maxima at 1-2 cm (Figure 3). Porewater Mn in the soluble size fraction (sMn) was also measured during the late spring season and had similar concentrations to dissolved Mn (dMn; Figure 4), indicating that dMn was entirely in reduced and soluble forms, consistent with the reductive dissolution of Mn(IV) following nitrate consumption.

Porewaters had similar depth-profiles for Fe concentration across all cores in both late spring and late summer (Figure 3; additional profiles are displayed in the supplementary information). Dissolved Fe was low at the surface (0.3 to 13 µM, 0-1 cm), and steadily increased towards large sub-surface maxima (100 to 170 µM, 5-8 cm), before decreasing slightly further down-core (~ 80 µM, 12 cm depth). Generally, porewater total dFe equals dFe(II) within sampling and analytical uncertainty. In addition, soluble Fe species (sFe), which were measured during the late spring conditions only, correspond with dFe concentrations within analytical uncertainty (Figure 4). However, surface and sub-surface dFe(II) concentrations were greatest in the late spring. Sub-surface dFe(II) maxima were 150 ± 20 µM (n = 3) in the late spring compared to 110 ± 10 µM (n = 3) in late summer conditions. Uppermost surface porewater dFe(II) concentrations were significantly elevated in late spring conditions (5 to 13 µM) compared to late summer conditions (0.3 to 1.2 µM; Figure 5). Concentrations decreased by 2-5 orders of magnitude in core top waters (14 to 21 nM; Figure 3; Table S4), relative to dFe in surface porewater, and decreased further into

bottom waters approximately 10 m above the seafloor (5.4 to 10 nM; Figure 3; Table S4; Figure 6; Table S5).

The isotopic composition of dFe (δ^{56}dFe) in porewater depth-profiles was similar in both seasons, ranging from -0.6 ‰ at 10-12 cm, to -3.0 ‰ in uppermost sediments – comparatively lighter than core top water and bottom waters, where δ^{56}dFe values ranged from -1.0 to -0.1 ‰ (Figure 3).

Porewater sulphide (H_2S) was below the limit of detection (< 1 µM) in our samples. By proxy, the abundance of dFe(II) in our deepest porewaters is also consistent with the absence of any substantial sulphate reduction and production of sulphide, and even trace amounts of H_2S below our detection limit would likely have already been titrated as Fe-sulphide by the excess of dFe(II).

Easily leached forms of Fe and Mn were consistently higher in surface sediments above dissolved sub-surface maxima during both seasons (Figure 3), and indicate a significant fraction of porewater Fe and Mn entrapment must be forming these authigenic solid-phases (Figure 3). Ascorbic acid released Fe (Fe_{asc}) was highest in surface sediments (up to 520 µg/g) and decreased down-core to ~150 µg/g. Trends for ascorbic released Mn (Mn_{asc}) were similar (surface up to ~35 µg/g decreasing to ~5 µg/g at depth). The H-HCl leach performed in the surface 1 cm of sediment resulted in a similar Fe release to that of the ascorbic acid leach. However, the H-HCl leach removed significantly more Mn (up to 120 µg/g) compared to the ascorbic acid leach.

Water column dFe(II) at our study site was also found to increase significantly towards the seafloor from < 15 pM at < 30 m (~75 m above the sea floor, asf) to 280 pM at 97 m (10 m asf) when measured between our sampling seasons, in July 2015 (Figure 6). Furthermore, Fe(II) represents ~ 4 % of the total dFe pool in these bottom waters, and is suggestive of a benthic source of dFe(II) and dFe to the water-column.

The air-tight incubation of water overlying sediment cores resulted in substantially elevated dFe(II) and dFe concentrations in the late spring (up to 225 and 232 nM, respectively), whilst in late summer much lower concentrations of dFe(II) and dFe were detected (on average 12 and 28 nM, respectively; Figure 7). During the subsequent

ventilation of these incubated core top waters in the late spring, dFe(II) concentrations decreased 10-fold after 150 minutes, but after nearly 500 minutes dFe(II) and dFe persisted at elevated concentrations similar to the late summer experiment (12 and 33 nM, respectively). Ventilation of core top water in the late summer produced no impact on dFe(II) or dFe concentrations in core top waters (Figure 7). The pH was monitored during the summer experiment and did not vary significantly (7.73 ± 0.05, 1SD, n = 2).

Further, Fe(II) oxidation experiments were designed to compare Fe(II) oxidation kinetics from core top waters in contact with sediments, bottom water isolated from sediments, and theoretical rates (Figure 8). All waters exhibited Fe(II) oxidation rates slower than theoretical predictions based on empirical constraints for seawater (Millero et al., 1987), with core top waters presenting the slowest rates of Fe(II) loss. Measurements of Fe(II) in diffusion experiments in the late summer showed no significant increase of dFe(II) or dFe over a period of 3 days (dFe(II) < 2 nM; dFe < 4 nM, Figure S2), which confirms the absence of significant inputs of Fe due to diffusion or handling in our shipboard experiments. The pH was monitored throughout the experiments and remained at 8.1 ± 0.3 (1SD, n = 5).

Discussion

Seasonal redox cycling of dFe and sFe in Celtic Sea shelf sediments

Oxygen penetration depths were most varied but, on average, shallowest in late spring (ranging 2.2-5.8 mm, Figure 2), which is consistent with wider spatio-temporal assessments of OPD in the Celtic Sea (Hicks et al. submitted). Most likely, this reflects the enhanced supply of organic carbon to the sediment and metabolic consumption of O_2, combined with enhanced macro benthic faunal activity at our study site. Higher rates of oxygen consumption and organic carbon oxidation are supported by modelled diffusion-consumption of O_2 (Figure 2). In addition, this hypothesis is supported by peak chlorophyll abundance, observed via MODIS satellites two weeks prior to our sediment sampling in late spring (Thompson et al. submitted), and particulate organic carbon concentrations in the

surface layers (0-10 cm) that are highest in late spring (1.25 %), and decrease by late summer (1.14 %) as bloom-derived carbon is decomposed (Figure S1).

Beneath the sediment surface, dissolved macronutrients (NO_3^-, NH_4^+) and metals (Fe, Mn) in porewaters follow their anticipated biogeochemical depth-distributions during early diagenesis (Froelich et al. 1979; Burdige 2006). Following the consumption of O_2, NO_3^- is reduced and transformed to NH_4^+, followed by the reduction of solid Mn and Fe oxides down-core and the release of their soluble reduced forms to porewaters (Figure 2). Assuming simple conversions between NH_4^+ and NO_3^- are a simplification of the true complexity of the benthic N-cycle. Briefly, the remineralisation of organic matter leads to the release of nitrogen in the form of NH_4^+, which is immediately oxidised to NO_3^- in the presence of oxygen, and which in turn is removed via denitrification and anammox in anoxic sediments below (e.g., Devol et al. 2015).

To date, there is little detailed knowledge of the redox state and size distributions of Fe in shelf sediment porewaters. Here we demonstrate that the proportion of porewater dFe as dFe(II) at our study site is > 85 % in the upper 3 cm and ~100 % in the ferruginous zone below (Figure 2). Thus, Fe(II) is supplied to porewater in the sub-surface (from the dFe(II) maxima, between 3 and 8 cm depth) and is prone to oxidative-removal towards the sediment surface, and most likely to sulphide-mineral trapping at deeper depths, resulting in the curvature typical of porewater Fe(II) profiles (Froelich et al., 1979; Severmann et al. 2006). Porewater profiles of Fe and Mn and their seasonal variations compare well to those in depositional areas of the southern and eastern North Sea (Slomp et al. 1997). Porewater dFe maxima are isotopically light (δ^{56}Fe -1.7 to -0.9 ‰), consistent with supply of dFe(II) from the dissimilatory reduction of Fe(III) oxide by bacteria (Severmann et al. 2006; Homoky et al. 2009; Henkel et al. 2016). In addition, our observations of dFe, δ^{56}dFe, dMn, nitrate and POC content in the Celtic Sea are similar to observed ranges in sediments from low-oxygen California-Oregon shelves (Severmann et al. 2006; Homoky et al. 2009; 2012) where benthic fluxes of isotopically light dFe to the ocean are observed (Severmann et al. 2010).

For the first time we have combined physicochemical Fe observations in porewater with speciation measurements. We show that porewater dFe(II) is almost entirely (> 85 %) in the soluble (< 0.02 μm) size range, and colloidal forms of Fe are largely absent under

these conditions (Figure 4). Similarly, porewater dMn(II) is also found in the truly soluble phase (100 % of dMn is < 0.02 um). The sFe forms may be simple ionic species, nano-particulate forms or may contain small ferrozine-reactive Fe(II) organic complexes. This contrasts with findings from deep sea sediments in the Crozet region presented in Homoky et al. (2009; 2011), where on average 80 % of Fe and 61 % of Mn was in the colloidal size fraction (0.02 to 0.2 µm). Porewater dFe mainly being in the reduced form in the shelf sediments studied here also means that there is no evidence for any significant concentrations of Fe(III) organic complexes as reported for anoxic porewaters in estuarine systems (Jones et al. 2011; Beckler et al. 2015).

Dissolved Fe generated in sediments and supplied to porewater will diffuse along its concentration gradient towards regions of reactive consumption or transport loss. Iron(II) oxidation in porewaters may be coupled to O_2 or NO_3^- reduction (Laufer et al. 2016). There are good empirical basis' to understand Fe(II) oxidation kinetics attributed to O_2 (Millero et al. 1987) and in the presence of NO_3^- (e.g., Gonzalez et al. 2010), previously explored in a study of benthic Fe flux (Homoky et al. 2012). However, the impact of enzymatic Fe(II) oxidation via NO_3^- reduction is still unclear. Near-surface gradients in dFe and dMn clearly indicate diffusion towards reaction in the surface oxic-layer, and potentially to the overlying water-column. A concomitant increase in sediment-leachable Fe and Mn is seen towards the sediment-water interface (Figure 3), and accounts for an important fraction of dissolved Fe and Mn removal in surface sediments. A similar inverse correlation between porewater dFe(II) and hydroxylamine-HCl leachable Fe has been observed in surface sediment from the North Sea, where the leachable Fe pool was also suggested to originate from sub-surface DIR (Henkel et al. 2016). The ascorbic acid leach extracts easily reducible ferrihydrite, which is the first amorphous Fe oxyhydroxide phase precipitated due to Fe(II) oxidation (Raiswell et al. 2010). The hydroxylamine-HCl leach extracts other reactive Fe phases that have been argued to be bioavailable, as well as ferrihydrite (Berger et al. 2008). Manganese seems to be trapped preferentially by materials released by the reducing hydroxylamine-HCl leach.

No sulphide was detected at any depths in our porewaters, and we observe negligible down-core enrichment of heavy Fe isotopes in porewater that would be indicative of removal to sulphides (Severmann et al. 2006). However, the gradual decrease in dFe(II)

below its maximum (Figure 3) most likely reflects downward diffusion as dFe(II) is converted to FeS in an underlying sulphate-reducing zone (Froelich et al. 1979).

The near-surface oxidation of Fe(II) to Fe(III) and the subsequent formation of Fe(III) oxides, is understood to preferentially incorporate heavier isotopes into authigenic Fe(III) phases, leaving behind lighter Fe(II) (e.g., Welch et al. 2003). Accordingly, a trend towards lower porewater δ^{56}Fe is observed from ~6 cm depth (~ -1.0 ‰) towards the sediment surface (~ -3.0 ‰) during both seasons, indicative of oxidative Fe(II) removal, and recycling during DIR (Severmann et al. 2006; Homoky et al. 2009). A return to higher porewater δ^{56}Fe in the uppermost sediment layer was observed during late spring and similar trends have been observed in sediment cores collected from shelf-slope sediments in the South East Atlantic (Homoky et al. 2013) and in the North Sea (Henkel et al. 2016). Henkel et al. (2016) reason that oxidative precipitation of Fe preferentially removes light isotopes, as proposed by Staubwasser et al. (2013), due to environmental variances in kinetic and equilibrium isotope fractionation processes compared to experiments (e.g. Welch et al., 2003). Whereas Homoky et al. (2013) reasoned that a transition to higher δ^{56}Fe towards the sediment surface resulted from mixing with an isotopically heavier and more stable Fe source, that has a relatively low dFe concentration. In both scenarios, a potential role for organic complexion of Fe exists. If such organic complexes were to stabilise a fraction of dFe across the surface oxidising zone of porewaters, the isotopic composition of the dFe pool might shift towards heavier isotopic compositions, which have been attributed to organic Fe-complexes (Dideriksen et al. 2008; Morgan et al. 2010), and would resist authigenic precipitation. Accordingly, our observed trend towards higher δ^{56}Fe extended from surface porewater into oxygenated core-top water and bottom water samples, while dFe concentrations steadily decreased (Figure 3).

Porewater dFe(II) was elevated in the surface (0-1 cm) during the late spring (4.5 to 13.4 µM, *n* = 3) compared to late summer (0.3 to 1.2 µM, *n* = 3, Figure 5, Table S3), coincident with the shoaling of OPD, linked to the deposition of organic matter during the bloom. Such seasonal variations in dFe and dMn were also reported in the water column of the North Sea and attributed to bloom-promoted release from sediments (Schoemann et al. 1998). Unexpectedly, our observed late spring surface porewater dFe(II) values are in the

same range as surface sediment dFe concentrations (~ 7 µM) from the high-carbon accumulating and low-oxygen Oregon Shelf (120 m water depth, Homoky et al. 2009), where substantial benthic fluxes of dFe have been measured. Albeit, our reported values remain lower than surface sediments underlying near-anoxic waters (e.g. ~100 µM dFe(II), (Severmann et al. 2006; Severmann et al. 2010). Dissolved Fe concentrations in overlying bottom waters (20 nM, with 15 nM as dFe(II); Table S4) were 1-5 orders of magnitude lower than the upper centimetre of porewater, and even lower in bottom water 10 m above the seafloor (5 to 10 nM; Figure 3). The presence of Fe(II) ranged from ~ 70 % of dFe in directly overlying bottom water at our study site (Table S4) to ~ 4 % at 10 m above sea floor (Figure 6, Table S5), indicating that a significant fraction of upward diffusing Fe(II) is able to escape the oxidative trap in the surface sediments and enter the water column.

Impact of water column oxygen on release of benthic Fe(II)

Large benthic fluxes of dFe to the water column are widely reported in oxygen deficient zones and are on the order of 100-1000 µmol m^{-2} d^{-2} (Homoky et al. 2016 and references therein). These observations enable an empirical assessment of the impact of oxygen concentration on the release of Fe(II) from seafloor sediments (Dale et al. 2015). Parts of the UK shelf, other than our study site, seasonally undergo modest periods of reduced-oxygen concentration (e.g., 160 - 200 µmol L^{-1}, compared to 280 - 310 µmol L^{-1} at other times of the year; Greenwood et al. 2010). To examine the likely impact of such changes in bottom water oxygen on the release of dFe from our study site, sediment cores and bottom water were sealed from the atmosphere, so that benthic respiration processes would draw down oxygen from the overlying water into the sediment. This resulted in similarly reduced dissolved oxygen concentrations at t = 0 hrs of ~150 and ~120 µM for late spring and late summer, respectively, but the accumulation of dFe in bottom waters was substantially different (Figure 7). High dFe concentrations (up to 240 nM) were measured in the late spring experiment, while in the late summer dFe concentrations only reached ~25 nM. This indicates that seasonal differences in near surface pore water dFe concentration (Figure 5) and OPD (Figure 2) are important controls on the release of dFe to bottom waters.

During the late spring, aeration of the incubated core top water induced rapid oxidation of Fe(II) and removal of dFe from solution (Figure 7). However, for both seasons

the residual concentration of dFe is in the range 25-30 nM, of which 30-50 % is present as Fe(II) despite reaching saturated oxygen concentrations – roughly 10 times greater than dFe concentrations reported for bottom waters at this site (5.4 to 10 nM, ~10 m above seafloor; Figure 3; Table S4; Figure 6; Table S5). Seawater Fe(II) oxidation kinetics predict nearly all Fe(II) should be oxidised to Fe(III) in our experiments in just a few minutes (Millero et al. 1987) and for this reason it has been generally assumed that oxic shelves are not a significant source of Fe to the overlying water column. However, the observation of Fe(II) present in oxic waters over a period of > 2 days suggests that rapid oxidation and fallout of Fe oxides is inhibited, due to some sort of Fe(II) and Fe(III) stabilisation. It is possible that organic carbon present during the late spring period, not only enhances the release of dFe, but also enhances the formation of organic ligands that are able to bind with Fe(II) and Fe(III) and serve to reduce the oxidative removal of dFe.

Fe(II) oxidation kinetics in core-top and water column seawater

The oxidation kinetics of Fe(II) were investigated in water column samples and in seawater overlying sediment cores (Figure 8). Oxidation rates in core top water were nearly twice as slow as in bottom waters, which themselves were more than 5 times slower than our empirical predictions (respective [Fe(II)] half-lives were 41, 23 and 3.8 minutes after Millero et al. (1987)). Further, the observed Fe(II) concentrations do not rigorously follow first order kinetics. Such behaviour has been observed in hydrothermal vent plumes, suggesting some stabilisation of the reduced form of Fe, possibly through organic complexation (Statham et al. 2005). Evidence for stabilisation of dFe(II) in marine systems by organic ligands has been observed in estuarine waters (Hopwood et al. 2015), in previous shelf sediment incubation experiments (Homoky et al., 2012), and in bottom waters adjacent to the continental margin (Bundy et al. 2014). Thus, most likely, the complexation of Fe to organic ligands plays an important role in stabilising sediment-derived Fe delivered to the water column. Laboratory studies have shown that a range of simple organic molecules can impact Fe(II) oxidation rates, and whilst some had no effect, others directly or indirectly slowed the net oxidation rate (Santana-Casiano et al. 2000). It is also possible that inorganic complexes such as sulphides could stabilize Fe(II) in solution in the form of Fe sulphide nanoparticles (Yücel et al. 2011), but evidence for this in shelf systems has not been demonstrated.

497 The high residual dFe(II) concentrations at the end of incubation experiments show
498 that something - most likely organic complexation - must routinely inhibit the oxidation of
499 Fe(II) and maintain a fraction of dFe(II) in solution. Core top waters sampled throughout our
500 study had consistently elevated dFe(II) and dFe concentrations (up to 14 and 21 nM,
501 respectively, Table S4). The diffusion experiment in the late summer showed no significant
502 increase or decrease in dFe(II) (0.8 ± 0.5 nM, *n* = 6) or dFe (2.8 ± 0.6 nM, *n* = 6) over a period
503 of 6 days in core-top water (Figure S2). Therefore, elevated dFe(II) and dFe concentrations
504 found in sampled core top waters must reflect an effectively stable form of Fe. Most
505 importantly, dFe(II) concentrations in core top water were substantially higher than dFe
506 concentrations in the overlying water column, indicating dFe(II) most likely originates from
507 the sediments and provides a source of dFe to the water column even in the late summer.

508 Organic complexation is also able to keep Fe(III) in solution above solubility-
509 controlled values, within the available ligand capacity. Evidence for Fe(III) ligand production
510 in sediments has been provided for an estuarine system (Jones et al. 2011). As the Fe(II) in
511 the proposed organic ligands is oxidised, it may remain associated with the ligand complex,
512 converting to Fe(III)-L complexes, which may be much stronger than Fe(II)-L complexes.
513 Alternatively, Fe(II) precipitation to Fe(III)-oxyhydroxide nanoparticles may constitute a
514 colloidal fraction of dFe with or without organic complexes (e.g., Raiswell and Canfield
515 2012).

516 Modelling of Fe(II) fluxes from sediments to an oxic water column

517 Organic complexes could inhibit the oxidative precipitation of dFe(II), and could therefore
518 increase the diffusive flux of dFe(II) across the oxic surface layer of shelf sediments to the
519 overlying water column. We consider the impact of organic complexes using a 1-
520 dimensional, steady-state, transport-reaction model to calculate diffusive fluxes of Fe(II)
521 from porewater to the water column. Our approach follows Raiswell and Anderson (2005),
522 which is used elsewhere to evaluate pore water fluxes of Fe(II) (Homoky et al. 2012;
523 Homoky et al. 2013; Wehrmann et al. 2014). To simulate the presence of organic ligands we
524 simply use a fraction (*f*) between 0 and 1 of the Fe(II) oxidation rate constant (*k)*, to
525 calculate the diffusive fluxes of Fe(II) based on site A sediment characteristics (Figure 9, see
526 supplementary information).

In the absence of any Fe(II)-stabilising ligands (f_k = 1) a diffusive flux of 24 µmoles Fe(II) m^{-2} d^{-1} is calculated from site A under late spring conditions, where OPD was 3.3 mm, pH 7.25 and near-surface Fe(II) concentration was 6.1 µM (averaged at 0.5 cm, *n* = 3). A smaller flux of 3.6 µmoles m^{-2} d^{-1} is calculated for late summer conditions (OPD = 4.1 mm, pH 6.88, Fe(II) = 0.9 µM, *n* = 3). If Fe(II) oxidation was prevented in the surface sediment (f_k → 0) these fluxes would increase by 30 and 8 % to 31 and 3.9 µmoles m^{-2} d^{-1}, respectively. Although we only have ionic diffusion coefficients available for our treatment of Fe(II)-Ligand complexes, Fe(II)-stabilizing ligands at Site A have a clear potential to impact diffusive fluxes. However, by stabilising dissolved species of Fe, their impact in the overlying water-column will likely be even more significant for benthic inputs. Diffusive fluxes of Fe(II) in the late spring period would provide up to 0.3 nmol L^{-1} d^{-1} throughout an evenly-mixed 110 m water column, compared to < 0.04 nmol L^{-1} d^{-1} in the late summer period. Our theoretical approach considers only diffusive transport, yet transfer of Fe(II) from pore waters could be further enhanced by advective transport due to physical mixing in the water-column, bio-turbation and -irrigation or anthropogenic disturbance to surface sediments.

A previous study of benthic Fe cycling in depositional areas of the North Sea found no dFe flux from sediments to overlying water using a steady state reaction-diffusion model, but found 20 to 210 µmoles m^{-2} d^{-1} when calculating diffusive dFe fluxes from measured porewater profiles modelling simple diffusion that ignored Fe(II) oxidation (Slomp et al. 1997). We can compare our diffusive Fe(II) fluxes from porewaters with those predicted by a recent global assessment of benthic Fe flux measurements from benthic chambers. Dale et al (2015) describes the dependence of benthic Fe flux on the rate of organic carbon oxidation in sediments and bottom water oxygen concentrations based on a compilation and regression of all known determinations. Where our organic C oxidation rates are calculated to be 8.6 to 11.9 mmol m^{-2} d^{-1} and bottom water oxygen is 267 to 252 µM, benthic Fe fluxes for our study site are estimated to be 8.0 µmoles m^{-2} d^{-1} in late spring and 5.5 µmoles m^{-2} d^{-1} in late summer – slightly higher than our late summer determination of 3.6-3.9 µmoles m^{-2} d^{-1}, but less than our late spring determination 24-31 µmoles m^{-2} d^{-1}. To a first approximation, this is a favourable comparison, and it is not unreasonable that individual study sites will have benthic Fe fluxes that deviate from the averaged

relationships described by Dale et al. (2015). However, it is also clear that well-oxygenated ocean margins have been largely absent from the compiled benthic Fe flux data used to parameterise ocean biogeochemical models to date (Homoky et al. 2016), hence there is potential for an underestimated contribution of dFe from oxic ocean margins.

Implications of benthic Fe(II) fluxes to an oxic water column

The dFe(II) stabilisation outlined above may enhance and maintain dFe(II) fluxes to the overlying water column. A study of the shelf and slope in the Bay of Biscay, south-west off the coast of Brittany found that labile dFe(II) species account for > 8 % of dFe species in bottom waters of the shelf break, and suggested that benthic processes (resuspension and diagenesis) represent important sources of dFe(II) and dFe, increasing the availability of Fe to microorganisms (Ussher et al. 2007). Elevated dFe(II) near the sea floor at Site A was also observed in July 2015 (Figure 6) and represents ~4 % of the dFe pool. The steep increase in dFe(II) concentrations towards the seafloor is consistent with our evaluation of a sedimentary source, although release of dFe(II) from the degradation of organic matter in the water column may also contribute to bottom water dFe(II) maxima.

Whilst there appears to be a low background diffusive input of Fe from the sediments throughout the seasons (Figure 9; Figure S2), the deposition of C in biogenic debris from the upper water column after the spring bloom is a major driver for additional inputs of Fe to porewaters, as was previously hypothesised (Schoemann et al. 1998). The degradation and turn-over of this organic material at the seafloor appears to happen within a 2-month period. Following release of Fe in the late spring, sediments gradually reset to pre-bloom conditions. This view of carbon flux to sediments being a major driver for iron release supports predictions from Elrod et al. (2004) and the revaluations by Dale et al. (2015). It is shown that the Fe flux is dependent on the position of the redoxcline within the sediment and the availability of organic material at the seafloor, with the stabilisation of dFe(II) by ligands acting as a further mechanism to enhance dFe transfer to the water column. The findings discussed here apply to cohesive shelf sediments. However, sandy mud only covers 0.8 % of the seafloor in the Celtic Sea. Sandy sediments, on the other hand, cover a large fraction of the seabed (16.5 %, Thompson et al. submitted) and are also affected by seasonal inputs of organic matter, where organic Fe complexation could

587 mediate benthic exchanges of Fe. This unconsolidated coarse sediment contains less organic
588 carbon, but is much more permeable and so may host important advection-dominated
589 exchange processes for dFe in shelf settings.

590 Based on our findings here, we suggest that temperate shelf seas equivalent to the
591 Celtic Sea need to be more explicitly represented in future ocean biogeochemical models,
592 where ligand-mediated benthic exchanges of Fe occur in response to seasonal
593 phytoplankton blooms. In such environments, Fe flux predictions based on previous benthic
594 chamber studies (e.g., Dale et al. 2015) might underestimate the true magnitude of
595 dissolved Fe input to the shelf seas. Although many sediment types across the Celtic Sea
596 receive seasonal inputs of organic matter, benthic Fe fluxes in cohesive and non-cohesive
597 sediments will be controlled by distinct diffusion-advection regimes for porewater solutes.
598 Animal activity, waves, tides and human-induced disturbances of shelf sediments will all
599 impact transport processes, but they are also ill quantified. An appraisal of exchange
600 processes and rates across coarser and more permeable sediments will support a more
601 rigorous scaling-up of our findings across the Celtic Sea, to quantify the impact of ligand-
602 mediated benthic fluxes to oxic shelf seas. Such a result, once seasonal perturbations to
603 benthic oxygen and to carbon dynamics and ligand-sustained fluxes of Fe are properly
604 accounted for, is likely to reveal that a larger amount of Fe is released from oxic shelf
605 sediments, which are estimated to typify most of the ocean-continent boundary, especially
606 in large areas of the Atlantic, Artic and Southern Oceans (Homoky et al. 2016), than
607 previously assumed.

608 Conclusions

609 Porewater dFe in cohesive sediments underlying an oxic shelf is mainly present as Fe(II) in
610 the soluble size fraction. This implies that porewater Fe(II) is in the ionic form or complexed
611 to ligands in the soluble size fraction. Porewater Fe(II) is produced at ~6 cm below the
612 surface via DIR, and is partially trapped in surface sediments as insoluble Fe(III) oxide phases
613 during upward diffusion, leading to low concentrations of residual dFe(II) in surface
614 porewaters with a characteristically light isotopic composition (δ^{56}Fe down to -3 ‰).

Even though large amounts of porewater dFe are lost to oxidation, the studies described here provide evidence for a significant release of dFe as Fe(II) from cohesive sediments underlying oxic waters on shelves in temperate systems. Stabilisation of dFe(II) in surface sediment porewaters appears to be an important factor for diffusion across the surface oxidizing layer of sediments, and most especially for the fate of dFe(II) species that are subsequently entrained in the water-column and contribute to elevated dFe concentrations on this oxic shelf. The deposition of phytoplankton debris at the seafloor provides a boost to the release of Fe through the decomposition and remineralisation of organic matter, as well as increased diagenetic release from sediments under changing redox conditions, in line with earlier work on sediment release of dFe(II) in response to carbon inputs (Elrod et al. 2004; Dale et al. 2015).

The work reported here provides a mechanistic explanation for the elevated dissolved water column Fe found overlying oxic shelves, relative to the open ocean. Given the global extent of oxic shelves, the work implies a larger shelf source of dFe to the ocean might exist than is predicted from existing compilations of benthic Fe fluxes that do not resolve the influence of organic complexation of Fe originating from shelf settings. Detailed studies of organic stabilisation processes in these and other ocean-sediment settings are required to improve our knowledge of the role and sensitivity of sedimentary sources of Fe linked to marine biogeochemical cycles.

Acknowledgements

This project was supported by Work Package 3 of the UK Shelf Sea Biogeochemistry Programme (NE/K001973/1 and NE/K001787/1), jointly funded by the Natural Environmental Research Council (NERC) and the Department for Environment, Food and Rural Affairs (Defra). The views expressed are those of the authors and do not necessarily represent those of NERC or Defra. W.B.H. was further supported by a NERC Fellowship (NE/K009532/1). The samples for this project were collected with the excellent support from captains, crew and NMF staff on the RRS *Discovery*. We are particularly grateful to fellow researchers within the SSB programme for providing assistance at sea and many discussions, which helped to shape the ideas presented in this manuscript. We express

special thanks to Carolyn Harris for analysing nutrient samples during cruise DY034. We are grateful for the constructive comments of two reviewers, which considerably increased the quality of this manuscript.

References

Beckler JS, Jones ME, Taillefert M (2015) The origin, composition, and reactivity of dissolved iron(III) complexes in coastal organic- and iron-rich sediments. Geochim Cosmochim Acta 152:72-88 doi:http://dx.doi.org/10.1016/j.gca.2014.12.017

Berger CJM, Lippiatt SM, Lawrence MG, Bruland KW (2008) Application of a chemical leach technique for estimating labile particulate aluminum, iron, and manganese in the Columbia River plume and coastal waters off Oregon and Washington. Journal of Geophysical Research: Oceans 113:n/a-n/a doi:10.1029/2007JC004703

Berner RA (1980) Early diagenesis: A theoretical approach. vol 1. Princeton University Press,

Boyd PW, Ellwood MJ (2010) The biogeochemical cycle of iron in the ocean. Nat Geosci 3 doi:10.1038/NGEO964

Bowie AR, Achterberg EP, Sedwick PN, Ussher S, Worsfold PJ (2002) Real-Time Monitoring of Picomolar Concentrations of Iron(II) in Marine Waters Using Automated Flow Injection-Chemiluminescence Instrumentation. Environmental Science & Technology 36:4600-4607 doi:10.1021/es020045v

Bundy RM, Biller DV, Buck KN, Bruland KW, Barbeau KA (2014) Distinct pools of dissolved iron-binding ligands in the surface and benthic boundary layer of the California Current. Limnol Oceanogr 59:769-787 doi:10.4319/lo.2014.59.3.0769

Burdige DJ (2006) Geochemistry of marine sediments. Princeton University Press, Princeton, NJ

Charette MA, Gonneea ME, Morris PJ, Statham P, Fones G, Planquette H, Salter I et al. (2007) Radium isotopes as tracers of iron sources fueling a Southern Ocean

670 phytoplankton bloom. Deep-Sea Res Part II-Top Stud Oceanogr 54:1989-1998
671 doi:10.1016/j.dsr2.2007.06.003

672 Cline JD (1969) Spectrophotometric Determination of Hydrogen Sulfide in Natural
673 Waters. Limnol Oceanogr 14:454-458

674 Conway TM, John SG (2014) Quantification of dissolved iron sources to the North
675 Atlantic Ocean. Nature advance online publication doi:10.1038/nature13482

676 Conway TM, Rosenberg AD, Adkins JF, John SG (2013) A new method for precise
677 determination of iron, zinc and cadmium stable isotope ratios in seawater by double-spike
678 mass spectrometry. Anal Chim Acta 793:44-52
679 doi:http://dx.doi.org/10.1016/j.aca.2013.07.025

680 Cullen JT, Chong M, Ianson D (2009) British Columbian continental shelf as a source
681 of dissolved iron to the subarctic northeast Pacific Ocean. Global Biogeochem Cycles 23
682 doi:10.1029/2008gb003326

683 Dale AW, Nickelsen L, Scholz F, Hensen C, Oschlies A, Wallmann K (2015) A revised
684 global estimate of dissolved iron fluxes from marine sediments. Global Biogeochem Cycles
685 29:691-707 doi:10.1002/2014gb005017

686 de Jong J, Schoemann V, Lannuzel D, Croot P, de Baar H, Tison J-L (2012) Natural iron
687 fertilization of the Atlantic sector of the Southern Ocean by continental shelf sources of the
688 Antarctic Peninsula. Journal of Geophysical Research: Biogeosciences 117:G01029
689 doi:10.1029/2011JG001679

690 de Jong JTM, Boye M, Gelado-Caballero MD, Timmermans KR, VeldhuiS MJW,
691 Nolting RF, van den Berg CMG et al. (2007) Inputs of iron, manganese and aluminium to
692 surface waters of the Northeast Atlantic Ocean and the European continental shelf. Mar
693 Chem 107:120-142 doi:10.1016/j.marchem.2007.05.007

694 Devol AH (2015) Denitrification, Anammox, and N_2 Production in Marine Sediments.
695 Annual Review of Marine Science, Vol. 7: 403 -423 doi: 10.1146/annurev-marine-010213-
696 135040

697 Dideriksen K, Baker JA, Stipp SLS (2008) Equilibrium Fe isotope fractionation between
698 inorganic aqueous Fe(III) and the siderophore complex, Fe(III)-desferrioxamine B. Earth
699 Planet Sci Lett 269:280-290 doi:10.1016/j.epsl.2008.02.022

700 Elrod VA, Berelson WM, Coale KH, Johnson KS (2004) The flux of iron from
701 continental shelf sediments: A missing source for global budgets. Geophysical Research
702 Letters 31 doi:10.1029/2004gl020216

703 Folk RL (1954) The distinction between grain size and mineral composition in
704 sedimentary rocks Journal of Geology 62:344-359

705 Froelich PN, Klinkhammer GP, Bender ML, Luedtke NA, Heath GR, Cullen D, Dauphin
706 P et al. (1979) Early oxidation of organic matter in pelagic sediments of the eastern
707 equatorial Atlantic: suboxic diagenesis. Geochim Cosmochim Acta 43:1075-1090
708 doi:http://dx.doi.org/10.1016/0016-7037(79)90095-4

709 González, AG, Santana-Casiano, JM, Pérez, N, González-Dávila, M, (2010) Oxidation
710 of Fe (II) in natural waters at high nutrient concentrations. Environ Sci Technol 44(21): 8095–
711 8101.

712 Greenwood N, Parker ER, Fernand L, Sivyer DB, Weston K, Painting SJ, Kroger S et al.
713 (2010) Detection of low bottom water oxygen concentrations in the North Sea; implications
714 for monitoring and assessment of ecosystem health. Biogeosciences 7:1357-1373
715 doi:10.5194/bg-7-1357-2010

716 Henkel S, Kasten S, Poulton SW, Staubwasser M (2016) Determination of the stable
717 iron isotopic composition of sequentially leached iron phases in marine sediments. Chem
718 Geol 421:93-102 doi:http://dx.doi.org/10.1016/j.chemgeo.2015.12.003

719 Hicks N, Ubbara G, Silburn B, Smith H, Kröger S, Parker R, Sivyer D et al. (submitted)
720 Oxygen dynamics in shelf seas sediments incorporating seasonal variability.
721 Biogeochemistry

722 Homoky W, Hembury D, Hepburn L, Mills R, Statham P, Fones G, Palmer M (2011)
723 Iron and manganese diagenesis in deep sea volcanogenic sediments and the origins of pore
724 water colloids. Geochim Cosmochim Acta 75:5032–5048 doi:10.1016/j.gca.2011.06.019

725 Homoky WB, John SG, Conway TM, Mills RA (2013) Distinct iron isotopic signatures
726 and supply from marine sediment dissolution. Nat Commun 4 doi:10.1038/ncomms3143

727 Homoky WB, Severmann S, McManus J, Berelson WM, Riedel TE, Statham PJ, Mills
728 RA (2012) Dissolved oxygen and suspended particles regulate the benthic flux of iron from
729 continental margins. Mar Chem 134:59-70 doi:10.1016/j.marchem.2012.03.003

730 Homoky WB, Severmann S, Mills RA, Statham PJ, Fones GR (2009) Pore-fluid Fe
731 isotopes reflect the extent of benthic Fe redox recycling: Evidence from continental shelf
732 and deep-sea sediments. Geology 37:751-754 doi:10.1130/g25731a.1

733 Homoky WB, Weber T, Berelson WM, Conway TM, Henderson GM, van Hulten M,
734 Jeandel C et al. (2016) Quantifying trace element and isotope fluxes at the ocean–sediment
735 boundary: a review. Philosophical Transactions of the Royal Society A: Mathematical,
736 Physical and Engineering Sciences 374 doi:10.1098/rsta.2016.0246

737 Hopwood MJ, Statham PJ, Skrabal SA, Willey JD (2015) Dissolved iron(II) ligands in
738 river and estuarine water. Mar Chem 173:173-182 doi:10.1016/j.marchem.2014.11.004

739 Johnson KS, Chavez FP, Friederich GE (1999) Continental-shelf sediment as a primary
740 source of iron for coastal phytoplankton. Nature 398:697-700

741 Jones ME, Beckler JS, Taillefert M (2011) The flux of soluble organic-iron(III)
742 complexes from sediments represents a source of stable iron(III) to estuarine waters and to
743 the continental shelf. Limnol Oceanogr 56:1811-1823 doi:10.4319/lo.2011.56.5.1811

744 Lacan F, Radic A, Labatut M, Jeandel C, Poitrasson F, Sarthou G, Pradoux C et al.
745 (2010) High-Precision Determination of the Isotopic Composition of Dissolved Iron in Iron
746 Depleted Seawater by Double Spike Multicollector-ICPMS. Anal Chem 82:7103-7111
747 doi:10.1021/ac1002504

748 Laufer K, Røy H, Jørgensen BB, Kappler A (2016) Evidence for the existence of
749 autotrophic nitrate-reducing Fe(II)-oxidizing bacteria in marine coastal sediment. Appl
750 Environ Microbiol 82:6120–6131 doi:10.1128/AEM.01570-16.

751 Marsay CM, Sedwick PN, Dinniman MS, Barrett PM, Mack SL, McGillicuddy DJ (2014)
752 Estimating the benthic efflux of dissolved iron on the Ross Sea continental shelf.
753 Geophysical Research Letters 41:7576-7583 doi:10.1002/2014GL061684

754 Millero FJ, Sotolongo S, Izaguirre M (1987) The oxidation-kinetics of Fe(II) in
755 seawater. Geochim Cosmochim Acta 51:793-801

756 Morgan JLL, Wasylenki LE, Nuester J, Anbar AD (2010) Fe Isotope Fractionation
757 during Equilibration of Fe-Organic Complexes. Environmental Science & Technology
758 44:6095-6101 doi:10.1021/es100906z

759 Nieuwenhuize J, Maas YEM, Middelburg JJ (1994) Rapid analysis of organic carbon
760 and nitrogen in particulate materials. Mar Chem 45:217-224
761 doi:http://dx.doi.org/10.1016/0304-4203(94)90005-1

762 Papadimitriou S, Kennedy H, Thomas DN (2004) Rates of organic carbon oxidation in
763 deep sea sediments in the eastern North Atlantic from pore water profiles of O-2 and the
764 delta C-13 of dissolved inorganic carbon. Marine Geology 212:97-111
765 doi:10.1016/j.margeo.2004.08.003

766 Radic A, Lacan F, Murray JW (2011) Iron isotopes in the seawater of the equatorial
767 Pacific Ocean: New constraints for the oceanic iron cycle. Earth Planet Sci Lett 306:1-10
768 doi:10.1016/j.epsl.2011.03.015

769 Raiswell R, Vu HP, Brinza L, Benning LG (2010) The determination of labile Fe in
770 ferrihydrite by ascorbic acid extraction: Methodology, dissolution kinetics and loss of
771 solubility with age and de-watering. Chem Geol 278:70-79
772 doi:10.1016/j.chemgeo.2010.09.002

773 Raiswell R, Canfield DE (2012) The iron biogeochemical cycle past and present.
774 Geochemical Perspectives 1:1-220 doi:10.7185/geochempersp.1.1

775 Santana-Casiano JM, Gonzalez-Davila M, Rodriguez MJ, Millero FJ (2000) The effect
776 of organic compounds in the oxidation kinetics of Fe(II). Mar Chem 70:211-222
777 doi:10.1016/s0304-4203(00)00027-x

778 Schoemann V, de Baar HJW, de Jong JTM, Lancelot C (1998) Effects of phytoplankton
779 blooms on the cycling of manganese and iron in coastal waters. Limnol Oceanogr 43:1427-
780 1441

781 Seeberg-Elverfeldt J, Schlüter M, Feseker T, Kölling M (2005) Rhizon sampling of
782 porewaters near the sediment-water interface of aquatic systems. Limnology and
783 Oceanography: Methods 3:361-371 doi:10.4319/lom.2005.3.361

784 Severmann S, Johnson CM, Beard BL, McManus J (2006) The effect of early
785 diagenesis on the Fe isotope compositions of porewaters and authigenic minerals in
786 continental margin sediments. Geochim Cosmochim Acta 70:2006-2022
787 doi:10.1016/j.gca.2006.01.007

788 Severmann S, McManus J, Berelson WM, Hammond DE (2010) The continental shelf
789 benthic iron flux and its isotope composition. Geochimica Et Cosmochimica Acta 74:3984-
790 4004 doi:10.1016/j.gca.2010.04.022

791 Sholkovitz ER, Boyle EA, Price NB (1978) The removal of dissolved humic acids and
792 iron during estuarine mixing. Earth Planet Sci Lett 40:130-136

793 Sigman DM, Boyle EA (2000) Glacial/interglacial variations in atmospheric carbon
794 dioxide. Nature 407:859-869

795 Slomp CP, Malschaert JFP, Lohse L, VanRaaphorst W (1997) Iron and manganese
796 cycling in different sedimentary environments on the North Sea continental margin.
797 Continental Shelf Research 17:1083-1117 doi:10.1016/s0278-4343(97)00005-8

798 Statham PJ, German CR, Connelly DP (2005) Iron(II) distribution and oxidation
799 kinetics in hydrothermal plumes at the Kairei and Edmond vent sites, Indian Ocean. Earth
800 Planet Sci Lett 236:588-596 doi:10.1016/j.epsl.2005.03.008

801 Staubwasser M, Schoenberg R, von Blanckenburg F, Kruger S, Pohl C (2013) Isotope
802 fractionation between dissolved and suspended particulate Fe in the oxic and anoxic water
803 column of the Baltic Sea. Biogeosciences 10:233-245 doi:10.5194/bg-10-233-2013

804 Stephens D (2015) North Sea and UK shelf substrate composition predictions, with
805 links to GeoTIFFs. doi:doi:10.1594/PANGAEA.845468

806 Stephens D, Diesing M (2015) Towards Quantitative Spatial Models of Seabed
807 Sediment Composition Plos One 10 doi:10.1371/journal.pone.0142502

808 Stookey LL (1970) Ferrozine - a new spectrophotometric reagent for iron. Anal Chem
809 42:779-& doi:10.1021/ac60289a016

810 Thompson CEL, Silburn B, Williams ME, Hull T, Sivyer D, Amoudry MO, Widdicombe S
811 et al. (submitted) An approach for the identification of exemplar sites for scaling up targeted
812 field observations of benthic biogeochemistry in heterogeneous environments.
813 Biogeochemistry

814 Ussher SJ, Worsfold PJ, Achterberg EP, Laës A, Blain S, Laan P, de Baar HJW (2007)
815 Distribution and redox speciation of dissolved iron on the European continental margin.
816 Limnol Oceanogr 52:2530-2539

817 Viollier E, Inglett PW, Hunter K, Roychoudhury AN, Van Capellen P (2000) The
818 ferrozine method revisited: Fe(II)/Fe(III) determination in natural waters. Applied
819 Geochemistry 15:785-790

820

821 Wehrmann LM, Formolo MJ, Owens JD, Raiswell R, Ferdelman TG, Riedinger N, Lyons
822 TW (2014) Iron and manganese speciation and cycling in glacially influenced high-latitude
823 fjord sediments (West Spitsbergen, Svalbard): Evidence for a benthic recycling-transport
824 mechanism. Geochim Cosmochim Acta 141:628-655 doi:10.1016/j.gca.2014.06.007

825 Welch SA, Beard BL, Johnson CM, Braterman PS (2003) Kinetic and equilibrium Fe
826 isotope fractionation between aqueous Fe(II) and Fe(III). Geochim Cosmochim Acta
827 67:4231-4250

828 Williams C, Sharples J, Mahaffey C, Rippeth T (2013) Wind-driven nutrient pulses to
829 the subsurface chlorophyll maximum in seasonally stratified shelf seas. Geophysical
830 Research Letters 40:5467-5472 doi:10.1002/2013gl058171

831 Woodward EMS, Rees AP (2001) Nutrient distributions in an anticyclonic eddy in the
832 northeast Atlantic Ocean, with reference to nanomolar ammonium concentrations. Deep-
833 Sea Res Part II-Top Stud Oceanogr 48:775-793 doi:10.1016/s0967-0645(00)00097-7

834 Yücel M, Gartman A, Chan cS, Luther III GW (2011) Hydrothermal vents as a
835 kinetically stable source of iron-sulphide-bearing nanoparticles to the ocean. Nature
836 Geoscience 4:367-371

837 List of Figures

838 Figure 1: Location of study site (black star) on a map of surface sediment types for the UK
839 shelf (inset) and Celtic Sea areas using simplified Folk textural classifications from mud (M)
840 through sand (S) to gravel (G), based on surface sediment maps of the British Geological
841 Survey (Folk 1954; Stephens 2015; Stephens and Diesing 2015). Site A is located in an area
842 of sandy mud (sM). Adapted from Thompson et al. (submitted).

843 Figure 2: Oxygen depth-profiles across the sediment-water interface at Site A during late
844 spring and late summer. Symbols show seasonally averaged O_2 measurements, and error
845 bars (2SD, *n* = 8-11) reflect natural variations down core. Analytical precision of individual
846 measurements is within the width of the symbols. Dashed lines reflect mean O_2 penetration
847 depths (OPDs) and grey bars their variability in each season (2SD, *n* = 8-11). Diffusive
848 boundary layers overlying the sediment water interface are observed to be 0.6 mm.
849 Modelled fits for oxygen depth-profiles are shown by the solid orange line; modelled
850 seasonally averaged O_2 consumption and proportional rates of seasonally averaged organic
851 C oxidation rates are presented (see text for more details).

852 Figure 3: Distribution of NO_3^-, NH_4^+, dMn, dFe, dFe(II), and δ^{56}Fe in porewaters and
853 distribution of Fe and Mn in easily reducible oxide phases in sediments. Parameters are
854 displayed for one selected core from each season. Concentrations of $N0_3^-$ and NH_4^+ in core
855 top water (bottom water sampled from sediment cores) are displayed above the sediment-
856 water interface; core top water $N0_3^-$ and NH_4^+ concentrations in late spring refer to
857 averaged values from Cores H and C (see supplementary information), as these data are not
858 available for this core. Diamond-shaped symbols above the sediment-water interface show
859 dFe concentrations and isotopic compositions from core top water and bottom seawater
860 (sampled ~10 m above the seafloor); note the change in axis for Fe concentrations in pore
861 water (μM) and bottom water (nM). All error bars (SD) are smaller than the symbols.

Figure 4: Distributions of soluble and dissolved Fe and Mn concentrations in porewaters during late spring. Error bars (1SD) are within marker shapes.

Figure 5: Average porewater dFe(II) concentrations during late spring and late summer. Averages are from three measurements of replicate sediment cores and error bars are the standard deviation of these three measurements, dominantly reflecting natural heterogeneity within the sediment. Between seasons porewater dFe(II) concentrations are indistinguishable from natural heterogeneity below 1 cm depth. However, during late spring, above 1 cm depth dFe(II) concentrations are significantly higher than during the late summer.

Figure 6: Distributions of a) dFe(II) and b) dFe and sFe in the water column at Site A during June 2015 (cruise DY033). The vertical dotted line indicates LOD for Fe(II) measurements and error bars indicate the standard deviation of each measurement.

Figure 7: Concentrations of dFe and dFe(II) in core top water over time during its reoxygenation after forcing decreased oxygen conditions in the late spring and the late summer. Error bars are standard deviations of single measurements.

Figure 8: Iron(II) oxidation kinetics in isolated bottom seawater and in bottom water overlying sediment cores (Core top water, replicates 1 and 2) in late summer conditions. Theoretical predictions (Millero et al. 1987) are displayed for comparison. The first-order rate constant, *k*, has been adjusted to find the best fit of data to a first-order rate (FOR) equation, $[Fe]_t = [Fe]_0 \times e^{-kt}$, from which the half-lives, $t_{1/2}$ (min), are displayed in plot (b).

Figure 9: Calculated diffusive fluxes of Fe(II) to bottom water. (a) Benthic fluxes calculated as a function of fractional (*f*) strength of the Fe(II) oxidation rate constant *k*. Where $f_k = 1$, *k* follows empirical dependencies of Fe(II) oxidation rate in seawater (Millero, et al., 1987). Where f_k is <1, Fe(II) oxidation is inhibited to simulate the presence of Fe(II)-stabilizing ligands. (b) Benthic Fe(II) flux normalized to its calculated value in the absence of any simulated ligands ($f_k = 1$). These theoretical considerations illustrate how benthic Fe(II) fluxes are greatest in late spring, and that ligands may serve to enhance the diffusive flux of dissolved Fe species released from sediments by up to 30 % in late spring and 8% in late summer.

Figure 10: Seasonal diffusive Fe(II) fluxes from the Celtic Sea Shelf and the proposed influence of stabilizing ligands. Calculated fluxes of Fe(II) to bottom water are indicated by arrow widths, and the potential influence of Fe(II)-stabilizing ligands by the density of green shading within arrows. Diffusive fluxes of Fe(II) which ignore the influence of ligands are smaller and correspond to minimum flux values described for each season. A shoaling of the oxygen penetration depth (OPD), increase in the surface porewater inventory of dFe(II) and an increase in the diffusive flux of dFe(II) to bottom waters coincides with the enhanced supply and decomposition of phytodetritus at the seafloor in late spring. An apparent 10-20 fold reduction in Fe(II) oxidation rates over empirical predictions observed in our study was attributed to the stabilizing influence of Fe(II)-complexing organic ligands at the seafloor. The extent to which ligands may moderate benthic Fe fluxes will further depend on their size, abundance, stability and diffusive properties, which were not determined in this study. Dissolved Fe delivered to bottom water will undergo continued oxidation of Fe(II) to Fe(III) in addition to particle-adsorption and aggregation processes. The true magnitude of dissolved Fe species released to bottom waters, will further reflect the influence of biological and physical disturbances to the sediment-water interface and transport mechanisms within the benthic boundary layer, which may further enhance exchange rates, but are neglected in our assessment.

Figure 1

Click here to download Figure Fig 1 map sediment type.png

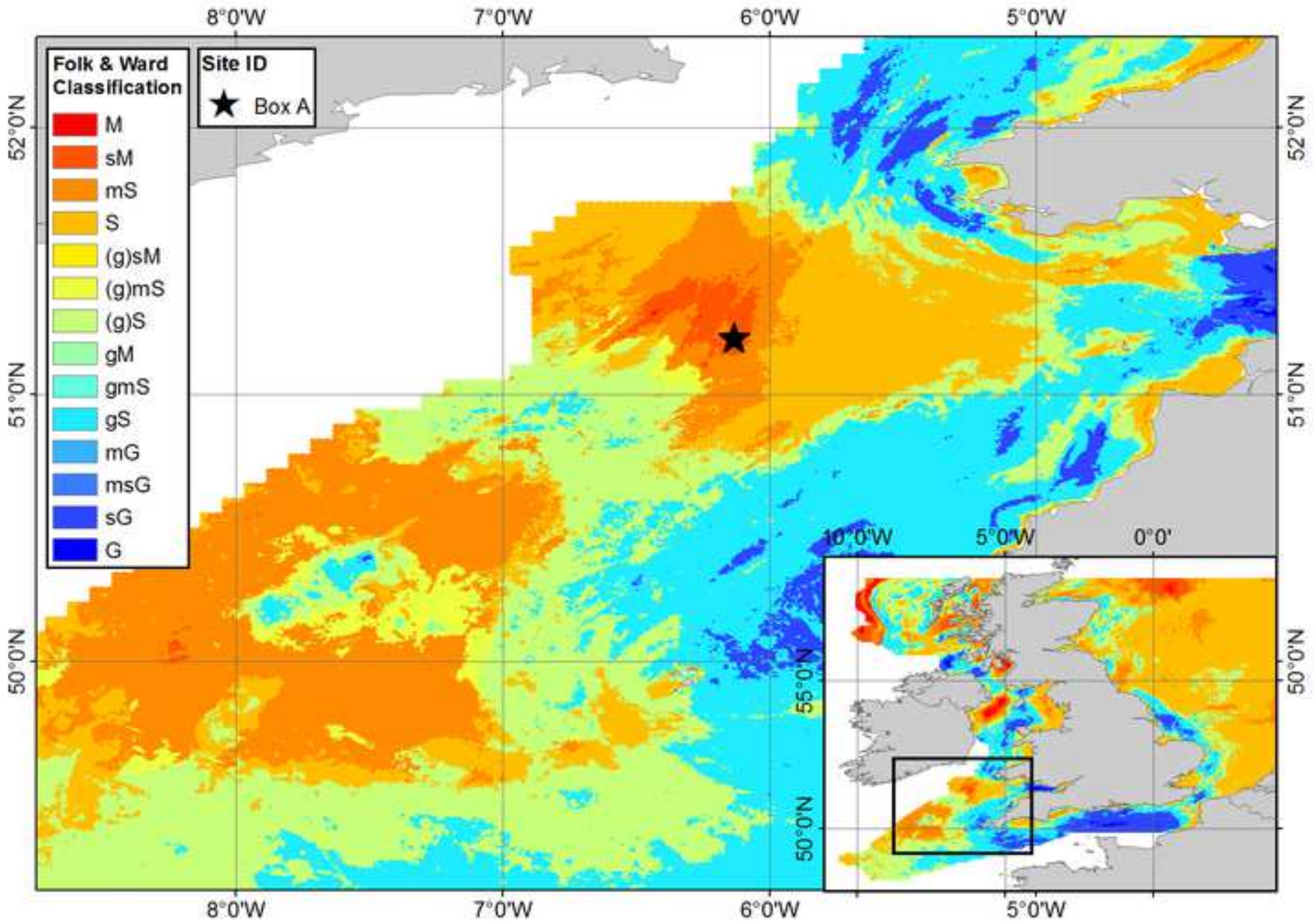

Figure 2

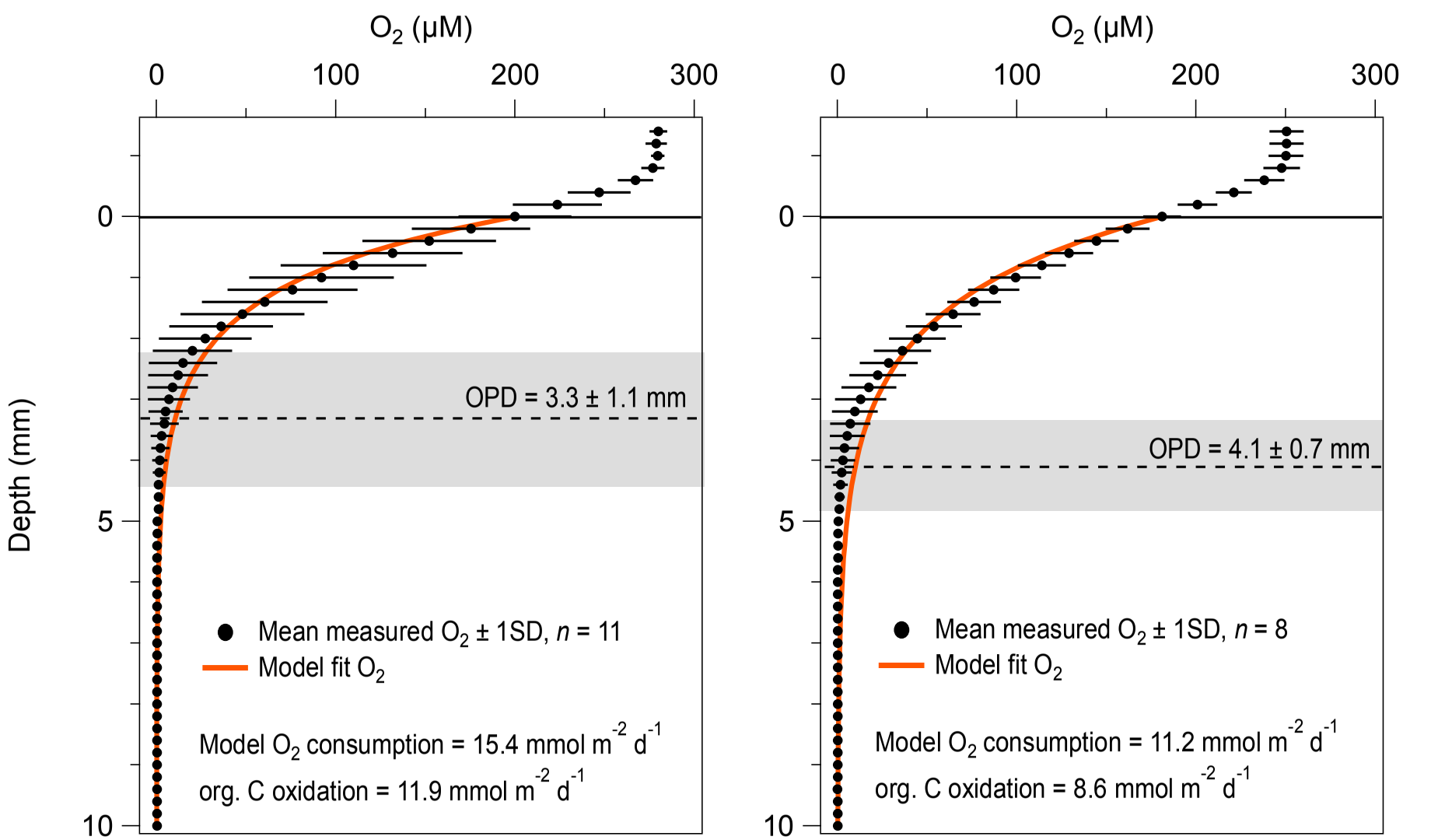

Figure 3

Click here to download Figure Fig 3 Porewater profiles grid.TIF

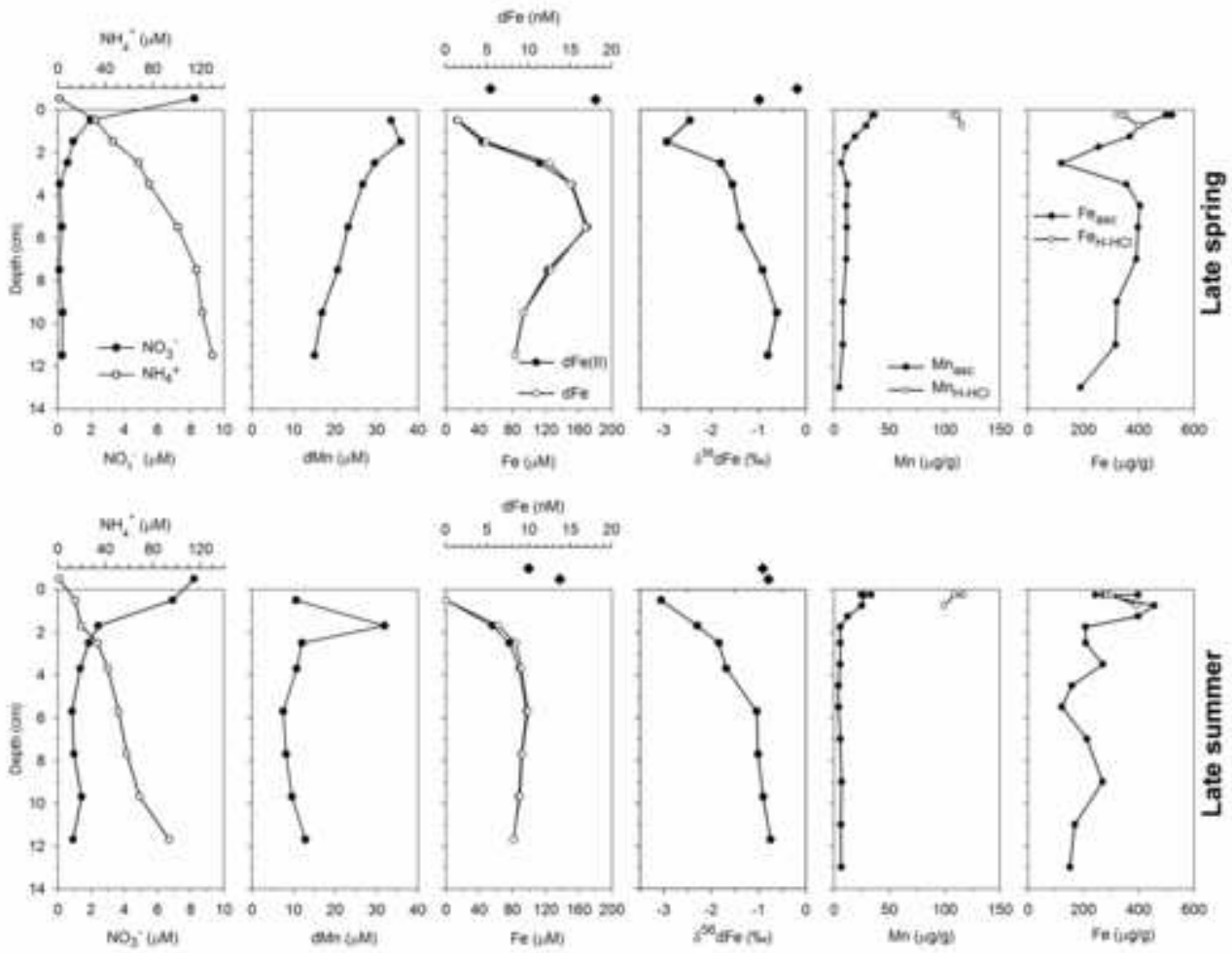

Figure 4

Click here to download Figure Fig 4 dissolved soluble Fe Mn.pdf

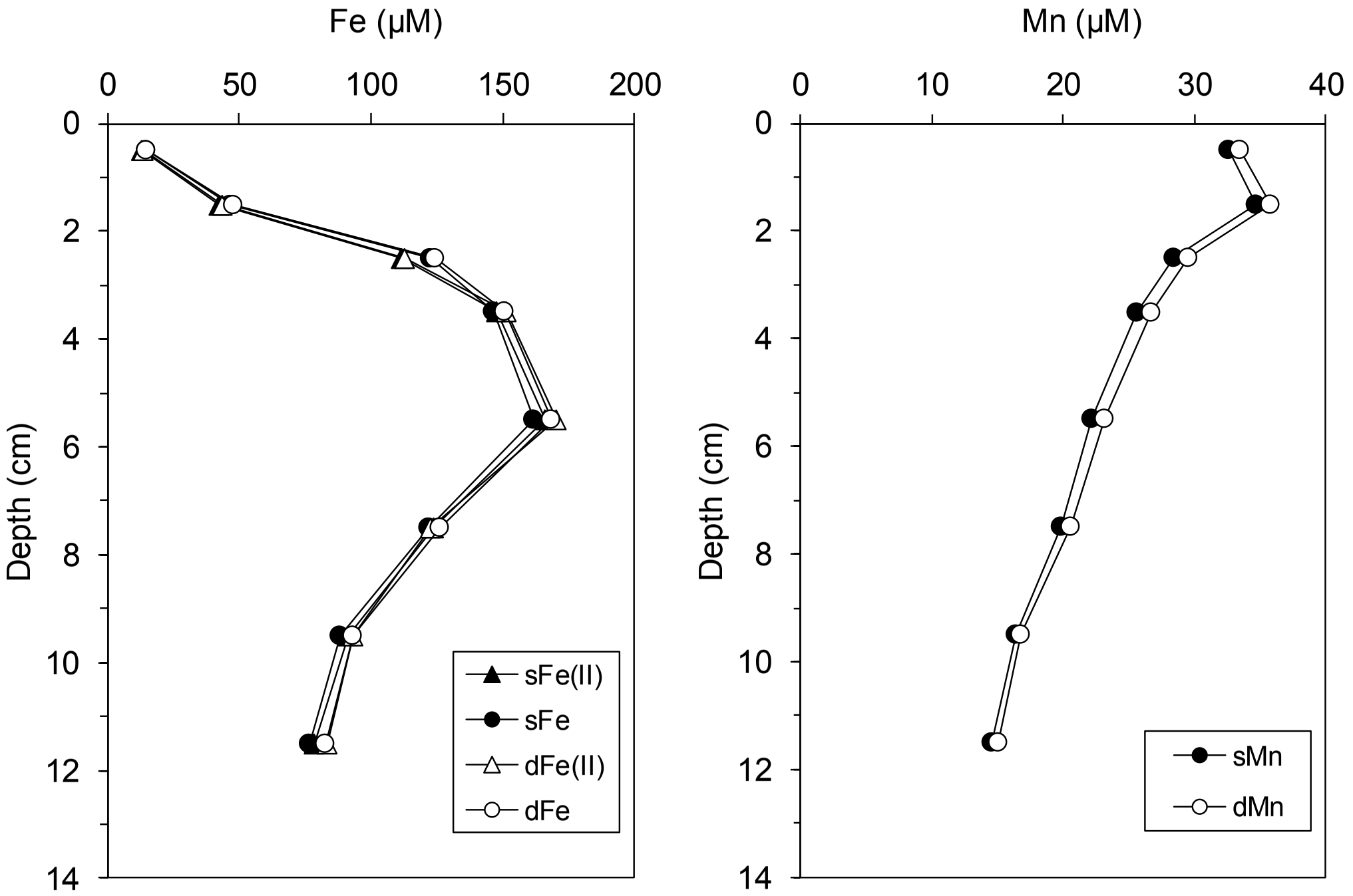

Figure 5

Click here to download Figure Fig 5 average PW dFe(II).pdf

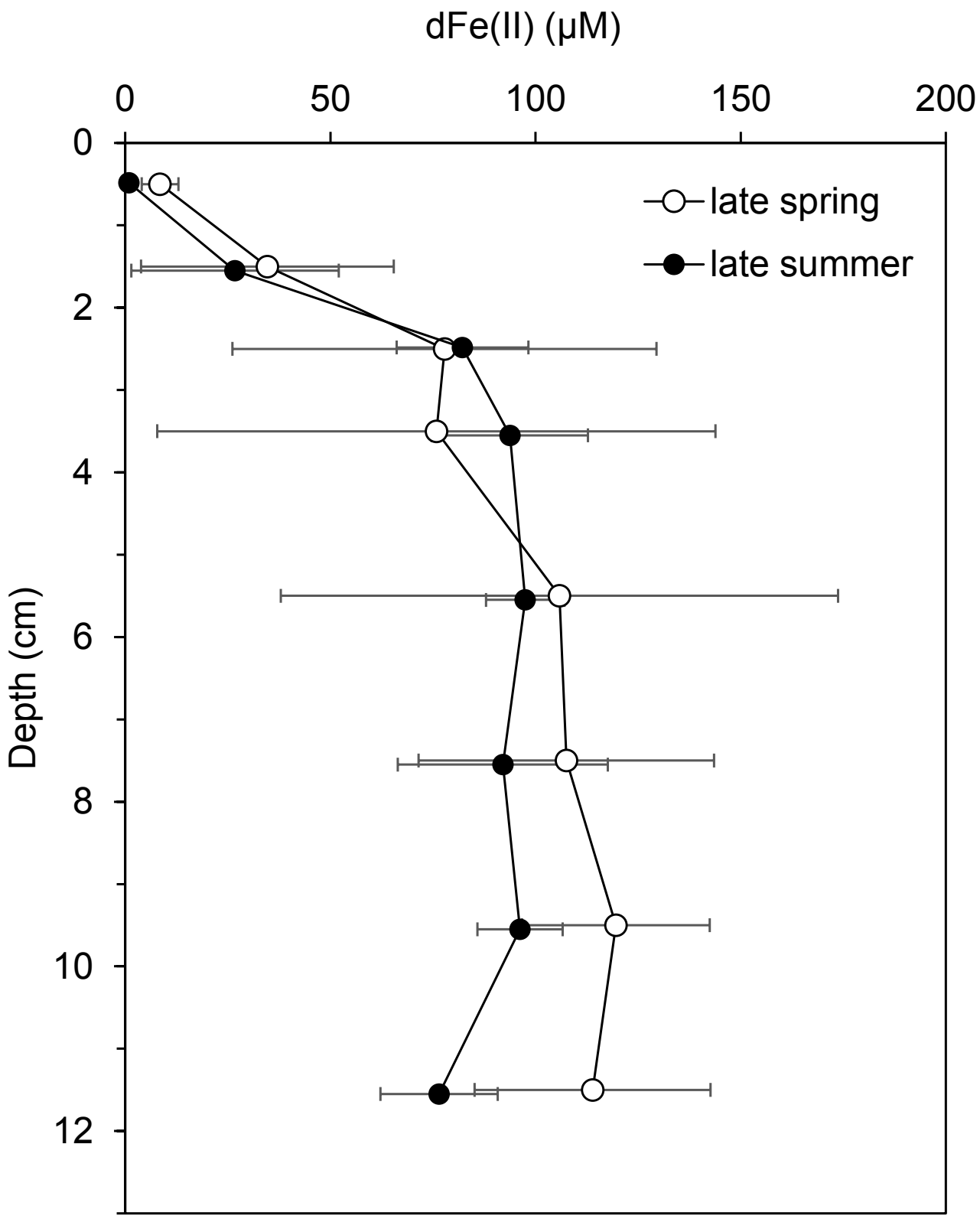

Figure 6

Click here to download Figure Fig 6 water column Fe.pdf

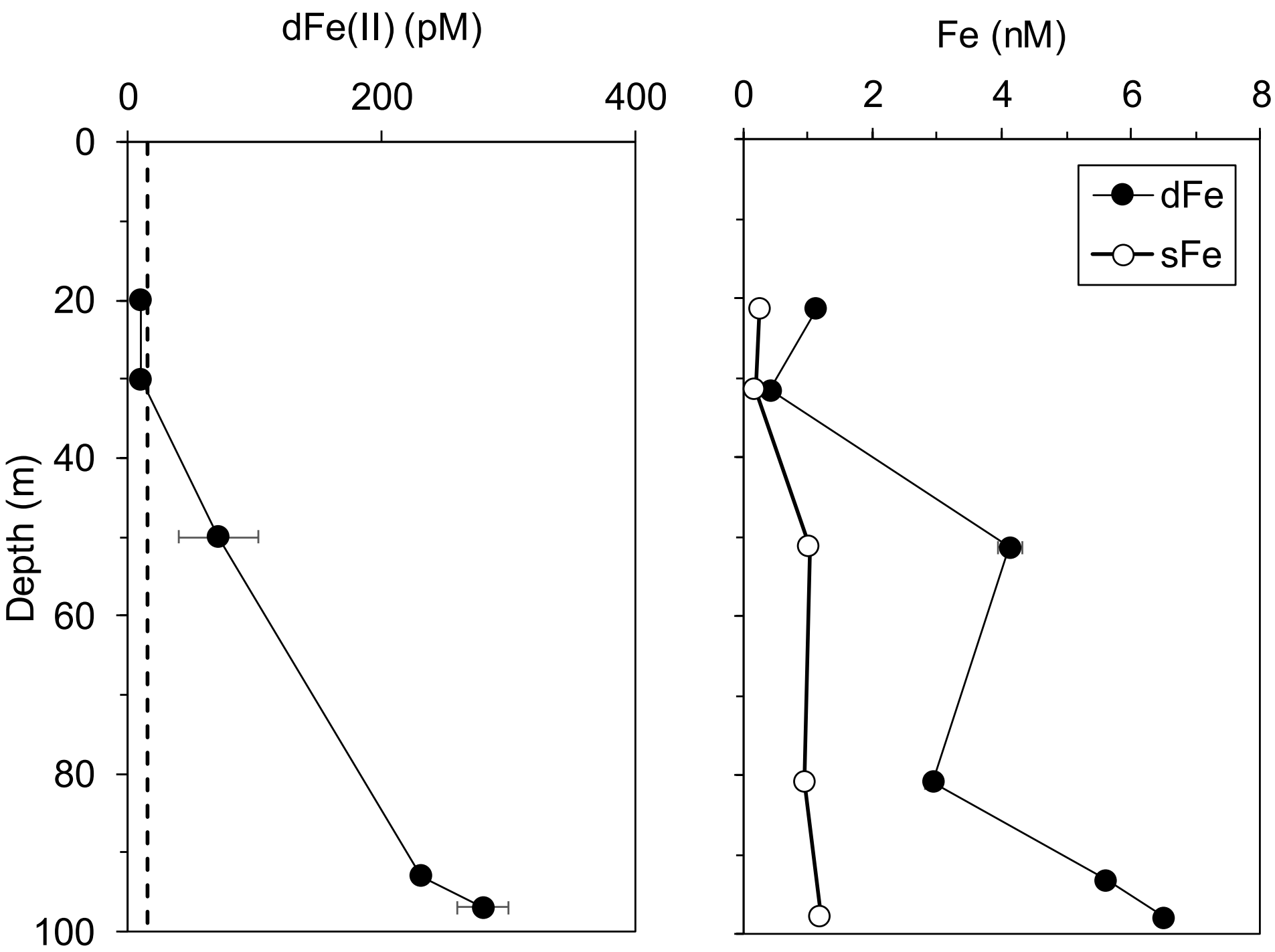

Figure 7

Click here to download Figure Fig 7 subox exp.pdf

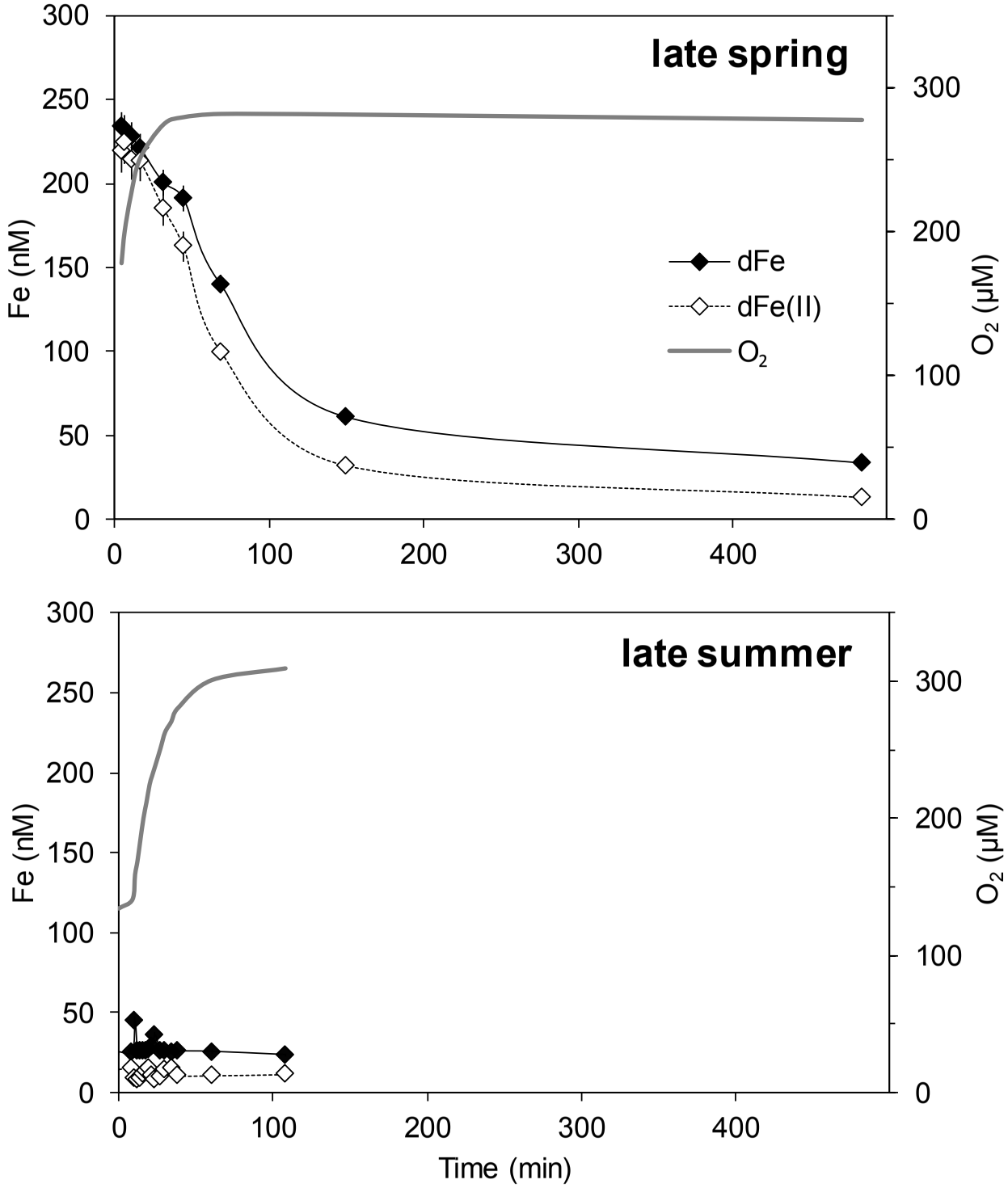

Figure 8

Click here to download Figure Fig 8 Fe(II) oxid exp.pdf

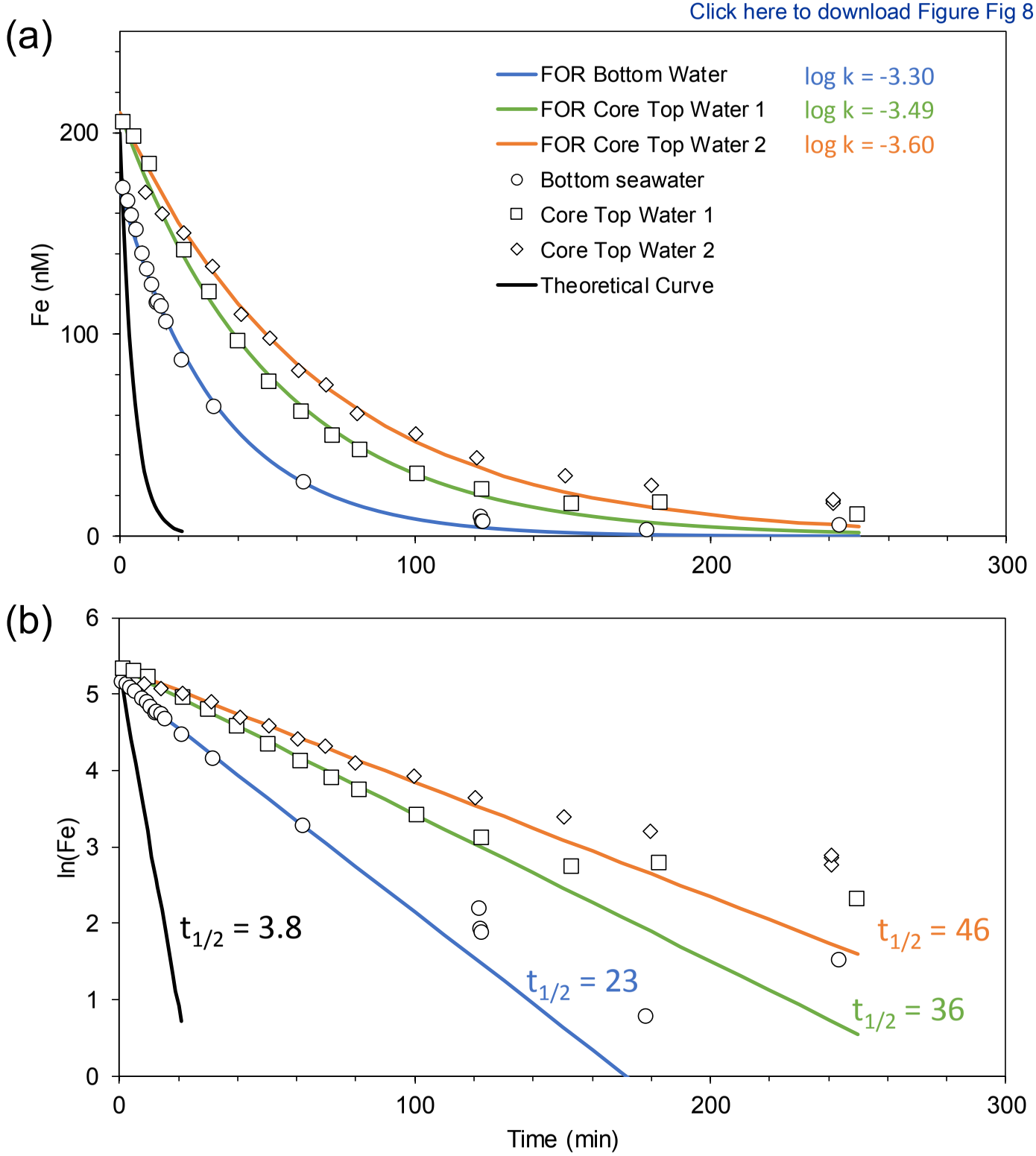

Figure 9

Click here to download Figure Fig 9 Fe flux model figure_v6.pdf

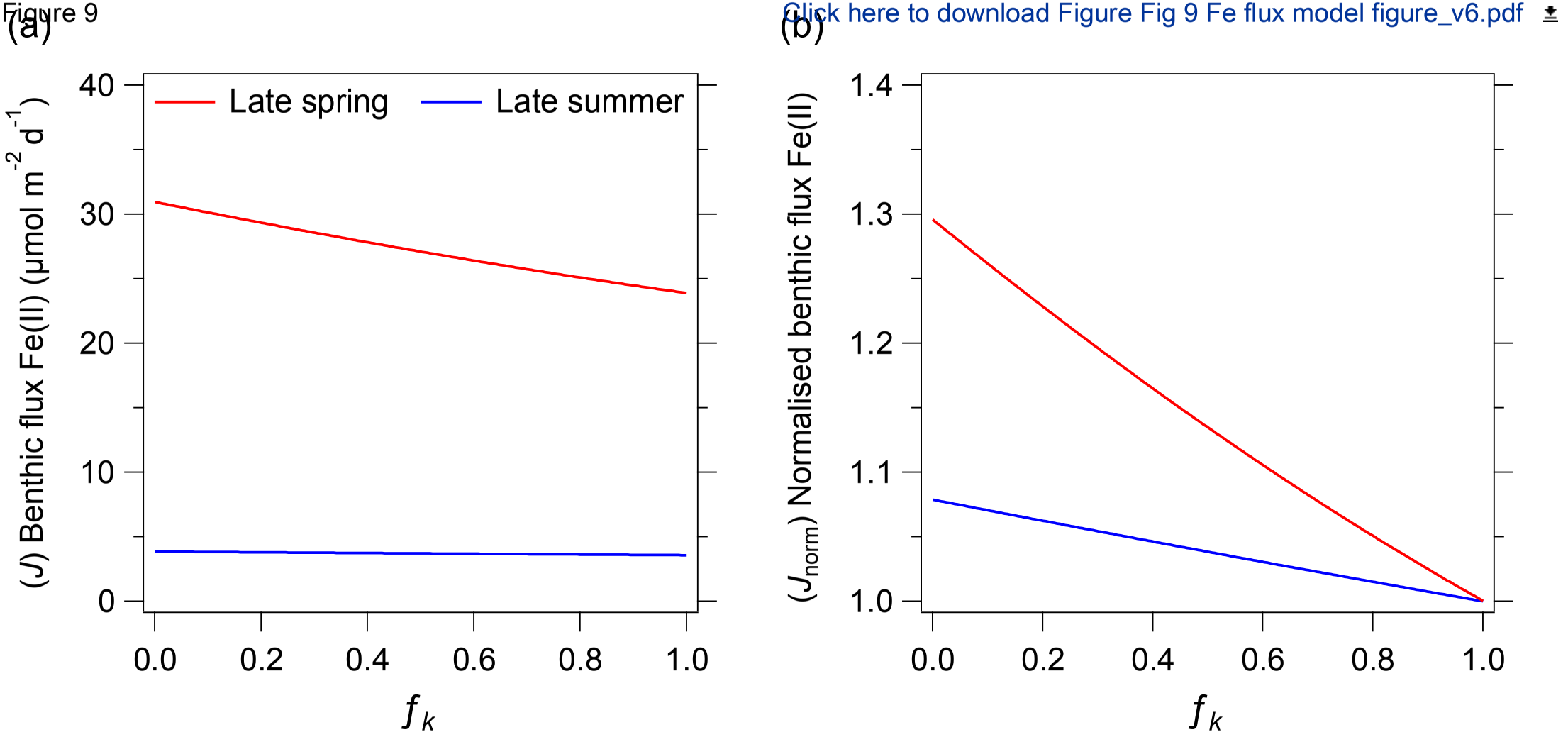

Figure 10

Click here to download Figure Fig 10 Draft final final summary figure.pdf

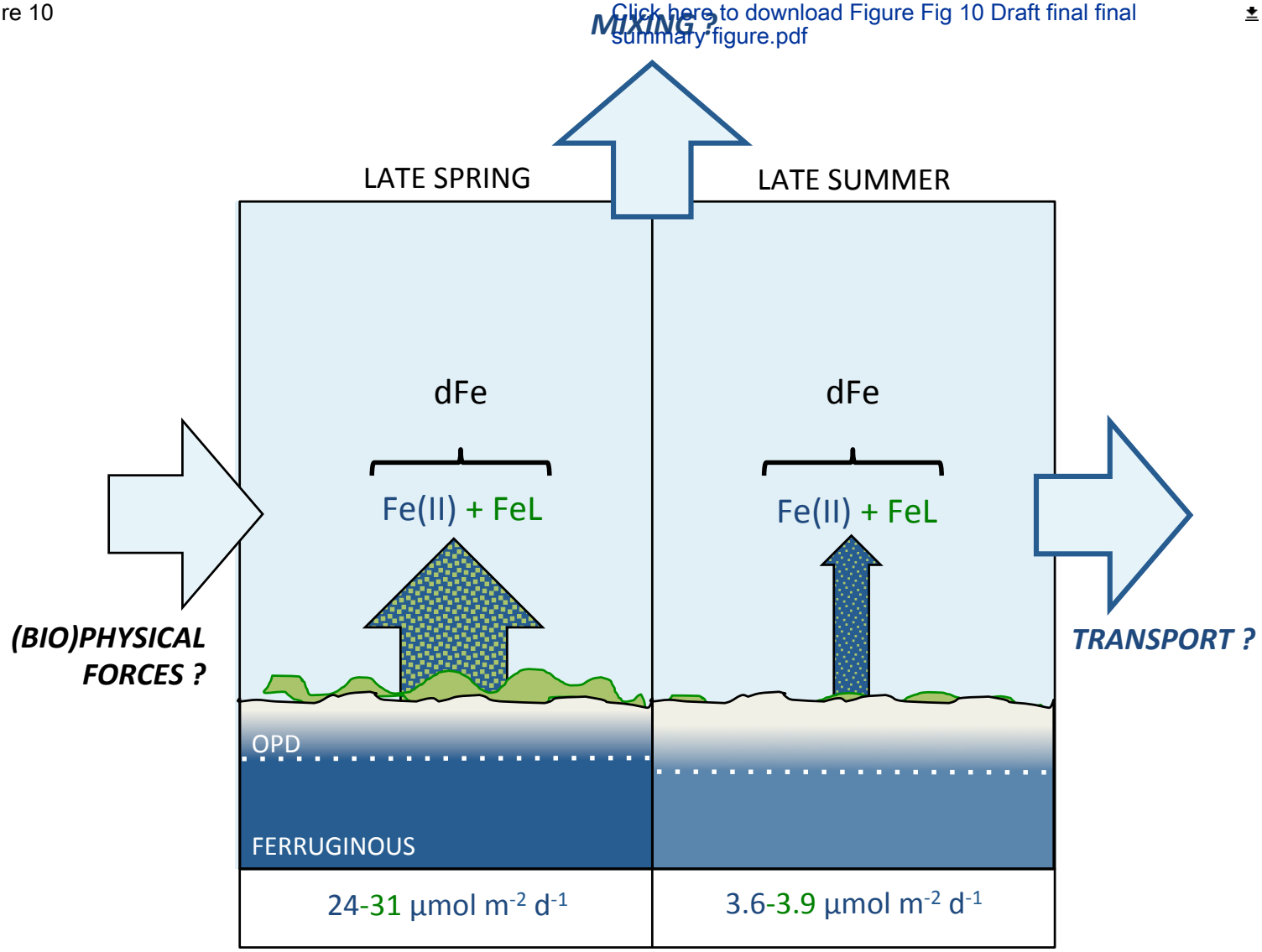

Supplementary Information

Stability of dissolved and soluble Fe(II) in shelf sediment pore waters and release to an oxic water column

Klar, J.K.[a,b*], Homoky, W.B.[c], Statham, P.J.[a], Birchill, A.J.[d], Harris, E.L.[a], Woodward, E.M.S.[e], Silburn, B.[f], Cooper, M.[a], James, R.H.[a], Connelly, D.P.[g], Chever, F[a], Lichtschlag, A.[g], Graves, C.[a]

[a] Ocean and Earth Science, University of Southampton, National Oceanography Centre, Southampton, SO14 3ZH, United Kingdom.
[b] Present address: LEGOS, Université de Toulouse, CNES, CNRS, IRD, UPS, 14 Avenue Edouard Belin, 31400 Toulouse, France.
[c] University of Oxford, Department of Earth Sciences, South Parks Road, Oxford, OX1 3AN, United Kingdom.
[d] School of Geography, Earth and Environmental Science, University of Plymouth, Drake Circus, Plymouth PL4 8AA, United Kingdom.
[e] Plymouth Marine Laboratory, Prospect Place, The Hoe, Plymouth, PL1 3DH, United Kingdom.
[f] Centre for Environment, Fisheries and Aquaculture Science, Pakefield Road, Lowestoft, NR33 0HT, United Kingdom.
[g] National Oceanography Centre, University of Southampton Waterfront Campus, European Way, Southampton, SO14 3ZH, United Kingdom.
*Corresponding author, email jessica.klar@legos.obs-mip

Analytical methods

Oxygen depth-profiles and time-series

A suite of Unisense O_2 micro sensors was used to measure the concentration of dissolved O_2 at 100-200 µm depth-intervals, and to monitor changes over time during Fe(II) oxidation experiments. Assessments of O_2 penetration depth (OPD, limit of O_2 detection ≤ 0.3 µM) were based on 2-4 profiles from each sediment core of the 3 collected in each season (Homoky et al. 2011; Homoky et al. 2013). Briefly, microsensors were calibrated using two end-point O_2 saturation values: 100 % (air saturated) and 0 % (N_2-flushed/O_2-purged or dithionite) seawater solutions were matched in temperature and salinity to bottom waters. Oxygen saturation was converted to molarity following its empirical dependence on salinity and temperature using SensorTracePro software.

Ship-board Fe(II) and total Fe analyses

The concentrations of Fe species - Fe(II) and Fe(II) plus Fe(III) (hereafter total Fe) – were determined in the dissolved and soluble size fractions of porewater samples using the Fe(II)-complexing ferrozine ligand (Sigma-Aldrich). The absorbance of the Fe(II)-ferrozine complex was measured spectrophotometrically at 562 nm before and after reduction of Fe(III) to Fe(II) by ascorbic acid (Sigma-Aldrich, TraceSELECT®) to determine respective Fe(II) and total Fe concentrations (Stookey 1970; Viollier et al. 2000). For sub-surface porewaters, where Fe concentrations were expected to be >1 µM, a 0.5 ml subsample was pipetted into 1.5 ml of 2 mM Ferrozine for Fe(II), and into 1.5 ml of 2 mM Ferrozine plus 0.2 ml of 10 mM ascorbic acid for total Fe. For surface porewaters and incubation experiment samples, where Fe concentrations were expected to be < 1 µM, a 1 ml subsample was pipetted into 100 µL of 5 mM Ferrozine in 1 M ammonium acetate buffer for Fe(II), and into an equal amount of Ferrozine-buffer plus 100 µL 10 mM ascorbic acid for total Fe. Concentrations > 1 µM were analysed in a 1 cm quartz cell on a spectrophotometer (ATI Unicam 8625). Concentrations < 1 µM were measured on a 250 cm 3000 Series Liquid Waveguide Capillary Cell (LWCC, World Precision Instruments) coupled to a tungsten LS-1 light source (Ocean Optics) and a USB4000 fibre optic spectrometer (Ocean Optics) (Waterbury et al. 1997). Fe(II) standards were prepared by diluting ammonium iron(II) sulfate hexahydrate (Sigma-Aldrich, purum p.a. grade) to match the concentrations of chemicals in the samples. On the UV-vis spectrophotometer, the limit of detection (LOD, three times the standard deviation of the blank) was 0.3 µM Fe(II) and the blank was 0.25 µM Fe(II). The typical relative standard deviation (obtained by measuring replicates) was 2 % for > 10 µM and up to 5 % below 4 µM. For the LWCC, the LOD was 0.7 nM, the blank was 6 ± 4 nM and the typical relative standard deviation was < 5 %.

Analyses of labile Fe(II) in seawater samples

During cruise DY033 (11th July – 8th August 2015) water column samples were collected with a Ti-CTD. Cast subsamples for labile Fe(II) were transferred into acid-washed and pre-rinsed LDPE vials. The samples were filtered inline by peristaltic pumping directly through a syringe filter (0.2 µm-pore size, PES membrane, Nalgene), that had been flushed (1 hour) with filtered seawater, into a flow injection chemiluminescence (FI-CL) analyzer. Samples were

stored at 4 ^{o}C in the dark and analysis took place within 20 minutes of sampling. Labile Fe(II) was determined by inline solid phase preconcentration onto an 8-hydroxyquinoline resin at pH 5.2, followed by acid elution and luminol chemiluminescence detection (Bowie et al. 2002; Ussher et al. 2007). The analyser was preconditioned by multiple analyses of a 'control' seawater sample and blank injections.

Calibration was performed by standard additions of Fe(II) to pH adjusted filtered surface seawater (pH 5.2). The limit of detection of this method (defined as three times the standard deviation of the blank) was 15 pM Fe(II) and the blank was 25 pM Fe(II). The average relative standard deviation, obtained from triplicate analyses, for all samples above the LOD was 6.7 %. The measurement was termed ''labile Fe(II)'' because the exact speciation of the iron complexes is unknown, and the term Fe(II) may imply that only inorganic Fe(II) species were determined.

Fe isotope analyses

For isotopic measurements of Fe in seawater samples and core-top waters a two-step procedure was used (Lacan et al. 2010; Conway et al. 2013). For a target quantity of 200 ng Fe, samples were pre-concentrated using NTA Superflow resin (Quiagen), and then purified by anion exchange chromatography (using AGMP-1 resin, BioRad). Porewater samples contained sufficient Fe such that only the purification step was needed. Samples were then analysed on a Neptune *Plus* multi-collector inductively coupled plasma mass spectrometer (MC-ICP-MS) (Thermo Scientific) in high resolution mode. Mass fractionation was corrected by adding a ^{57}Fe/^{58}Fe double spike to samples prior to chemical processing. Isotope ratios are expressed in delta notation relative to the average value of the reference material IRMM-014 (Institute for Reference Materials and Measurements) determined during the same analytical session: δ^{56}Fe (‰) (= $[(^{56}Fe/^{54}Fe)_{sample}/(^{56}Fe/^{54}Fe)_{IRMM\text{-}14} - 1] \times 1000$). The procedural blank, determined on an Element 2XR ICP-MS (Thermo Scientific) was 4.3 ng Fe for the preconcentration step and 0.5 ng Fe for the purification step. The blank contributed < 4 % Fe to the sample. The Fe isotopic haematite standard ETH (Eidgenössische Technische Hochschule, Zürich) was analysed regularly during analytical sessions and was 0.52 ± 0.04 ‰ (2 SD, *n* = 38), compared to a consensus value of 0.52 ± 0.08 ‰ (2SD, *n* = 80; Lacan et al.,

2010). The analytical procedure was validated by taking aliquots of ETH reference material through the purification procedure (0.55 ± 0.05 ‰, 2 SD, *n* = 2).

Analyses of Mn concentrations in porewaters

Porewater Mn concentrations in soluble and dissolved size fractions were determined in diluted samples (20 to 100 fold in 0.3 M thermally distilled HNO_3) on a quadrupole ICP-MS (X-Series, Thermo Scientific). The blank was < 0.8 nM, the LOD was 0.2 nM and the typical relative standard deviation was 2 %.

Leachable Fe and Mn phases in sediments

In order to examine phase associations of Fe and Mn in solid sediment phases, two leaching schemes were applied to one core per season. An ascorbic acid leach (Raiswell et al. 2010) was applied, which extracts the easily reducible oxide phase such as amorphous ferrihydrite but not the more crystalline oxide phases. Additionally, an acetic acid-hydroxylamine-HCl (H-HCl) leach (Berger et al. 2008) was also used to extract other amorphous oxide phases as well as ferrihydrite. For detailed method descriptions, the reader is referred to the references cited above. Fe and Mn in the leach solutions were determined using an inductively coupled plasma optical emission spectrometer (ICP-OES, iCAP6000 Series, Thermo Scientific). For Fe, the blank was < 0.06 µg/g, the LOD was < 4 µg/g and the typical standard deviation was ~20 µg/g. For Mn, the blank was < 0.02 µg/g, the LOD was < 0.6 µg/g and the typical standard deviation was 4 µg/g.

Nutrient and sulphide analyses

Nutrient concentrations in water column samples, in sediment porewaters and experiments, were all analysed on board using a Bran and Luebbe segmented flow colorimetric auto-analyser (Woodward and Rees 2001). Sampling and handing techniques were carried out according the International GO-SHIP nutrient manual recommendations (Hydes et al. 2010). Nutrient reference materials (KANSO Japan) were run each day for quality control. The typical relative standard deviation was 2-3 %; and the limits of detection were 0.02, 0.01, and 0.05 µmoles L^{-1} for “nitrate plus nitrite”, nitrite, and ammonia, respectively. Nitrate was obtained by subtracting nitrite from the “nitrate plus nitrite” measurement. Sulphide was

measured using the colorimetric technique of Cline (1969), and the detection limit was 1 µM.

POC & PON in sediments

Particulate organic carbon (POC) and nitrogen (PON) were determined using a Carlo-Erba CHNOS analyser. The procedure followed Nieuwenhuize et al. (1994), in which the carbonate in samples contained in silver cups is removed by acidification with HCl before measuring POC, and inorganic C is given by the difference between a total C value and the POC measured. Precision was 6.6 % RSD at 1.5 % POC and 2.4 % RSD at 0.13 % PON. Estimated detection limit for C was 3.6 µg and all sample carbon contents were well above this value (Figure S1). Elemental Microanalysis Soil was used as a standard and monitored regularly.

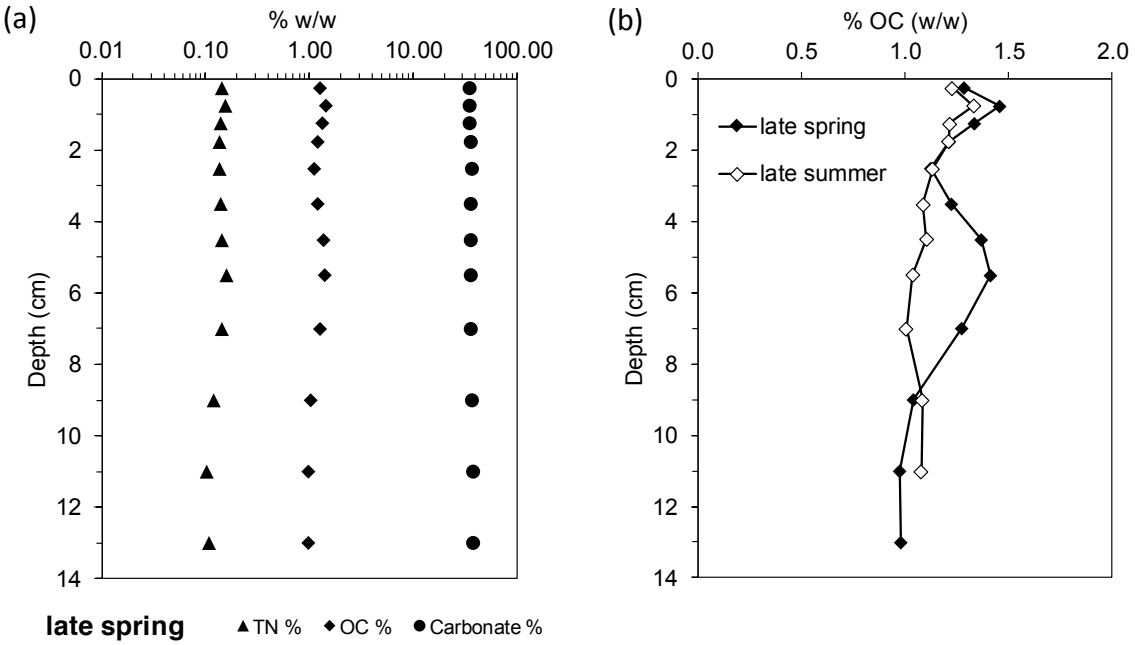

Figure S1: Distributions of total nitrogen (TN), organic carbon (OC) and carbonate during late spring conditions (a); and a seasonal comparison of the distribution of organic carbon (b) in sediments at Site A.

pH measurements in experiments

All pH electrodes were calibrated daily using a Certified Reference Material (TRIS pH buffer in synthetic seawater) supplied by Andrew Dickson, University of California (Nemzer and Dickson 2005; Silburn et al. submitted).

Benthic Fe diffusion experiment

Three replicate cores were collected from site I (muddy sand, ~ 50° 34.5557 N, 7° 6.3161 W, Thompson et al., submitted). Sediments at this site are characterized by a higher sand content, compared to Site A. A Milli-Q water rinsed control core tube containing no sediment was set up as a control. Original core top water was subsampled before carefully being syphoned off. A known amount (1 L) of clean unfiltered seawater (collected with the Ti-CTD at Site I) was slowly added to each of the 4 cores. This water had ~ 1 nM dFe and dFe(II) below LOD (< 0.7 nM). Core top water was kept oxygenated and in the dark at all times and was subsampled at several time intervals for dFe, dFe(II) and pH using Teflon tubing and a syringe. The experiment was carried out in a temperature-controlled lab at 11.5 to 11.7 °C.

The control core had dFe and dFe(II) concentrations below LOD, most likely due to adsorption onto the walls. Original core top water contained 10 ± 9 nM dFe and 8 ± 9 nM dFe(II) (Figure S2). After the replacement with clean water, dFe and dFe(II) concentrations were significantly lower and did not change significantly over time (average over 6 time points was 2.8 ± 0.6 nM dFe and 0.8 ± 0.5 nM dFe(II); Figure S2). The average water pH was 7.98 ± 0.01 (1SD, n = 4).

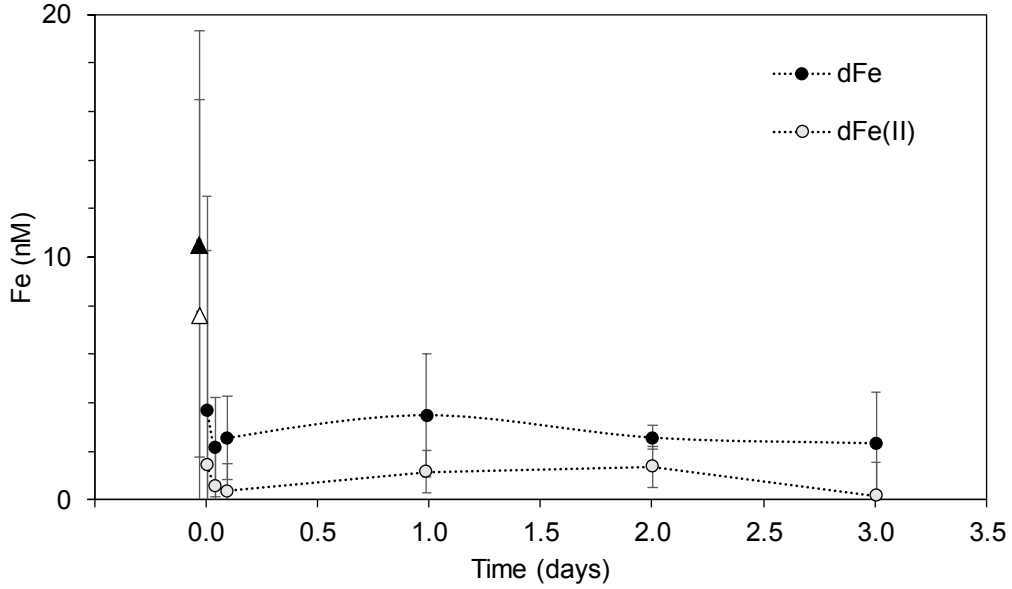

Figure S2: Concentrations of dFe(II) and total dFe in core top water, to mimic the diffusion across the sediment-water interface, carried out at Site I (muddy sand, Thompson et al., submitted) in late summer conditions. Original Core top water (represented by black and empty triangles for dFe and dFe(II), respectively) was exchanged with bottom water at time 0. Error bars represent the standard deviation of three replicate measurements in three replicate experiments.

Calculation of benthic Fe(II) flux from porewaters

We follow Raiswell and Anderson (2005) who describe the flux of Fe(II) to bottom water as a function of vertical diffusion and oxidative-loss in surface sediments beneath an oxygenated water column. This approach has previously been used to calculate the steady-state diffusive flux of dissolved Fe to oxygenated waters from subtropical, temperate and high-latitude ocean margin sediment pore waters (e.g., Homoky et al. 2012; Homoky et al. 2013; Wehrmann et al. 2014). For a consideration of the parameterisation of Fe(II) oxidation rate in these calculations (e.g. due to NO_3^-, pH) and an inter-comparison of the approach to Fe flux determinations by *in situ* benthic chambers, see Homoky et al. (2012). Equation S1 describes the vertical diffusive flux (J) of Fe(II) from sediment pore water to bottom waters in units of mol cm^{-2} s^{-1}:

$$J = \frac{\varphi(D_s k_1)0.5 C_p}{sinh[(k_1/D_s)0.5L]}, \qquad \text{(Eq. S1)}$$

where φ is sediment porosity (with assumed uniformity), L is the thickness (cm) of the oxygenated surface layer (equal to oxygen penetration depth plus diffusive boundary layer thickness), and C_p is the concentration (g cm^{-3}) of Fe(II) in the pore water beneath L.

The rate constant for Fe(II) oxidation is represented by k_1 (s^{-1}, Equation S2):

$$k_1 = k[O_2][OH^-]^2, \quad \text{(Eq. S2)}$$

and is a function of bottom water O_2 concentration (mol L^{-1}), pH, and a value k (s^{-1}) derived from the temperature, T, (°K) and salinity (I = ionic strength) dependence of Fe(II) oxidation rate in seawater (Equation S3) after Millero et al. (1987):

$$log\ k = 21.56 - \frac{1545}{T} - 3.29I^{0.5} + 1.52I, \quad \text{(Eq. S3)}$$

We also derive a diffusion coefficient of pore water Fe(II) in muddy shelf sediments after Raiswell and Anderson (2005) in Equation S4, where D_s ($cm^2\ s^{-1}$) is a function of φ, corrected for tortuosity, and temperature, T (°C):

$$D_s = \varphi 1.7(3.31 + 0.15T)10^{-6}. \quad \text{(Eq. S4)}$$

Simulated impact of Fe(II)-stabilising ligands on benthic Fe(II) flux

We consider the impact of Fe(II) stabilised by ligands (Fe(II)-L) present in pore water, on the steady-state diffusive fluxes of Fe from shelf sediments. In our assessment we must assume Fe(II)-L has a diffusion coefficient equal to ionic forms of Fe(II) in solution. Such a simplification of reality likely overestimates the true coefficient of Fe(II)-L diffusion. However, even though such properties are not truly known, comparatively large complexes of some other trace elements (e.g. Cu and Pb) are estimated to diffuse just ~25 % slower than free ions in solution (Phillips and Ellis 1970; Scally et al. 2006). In the absence of known values, and given that we observe dFe(II) almost entirely in a soluble size fraction, we consider an application of ionic diffusion coefficients in this context to be reasonable.

We simulate the presence of Fe(II)-L by inhibiting Fe(II) oxidation rates. To do so, we use a variable fraction (f) of k_1 from 1 towards 0, so Equation S1 becomes S5:

$$J = \frac{\varphi(D_s f k_1)0.5C_p}{sinh[(f k_1/D_s)0.5L]}. \quad \text{(Eq. S5)}$$

When f = 1, calculation of J using Equation S5 is identical to that made by S1. When f = <1, k_1 is reduced, inhibiting the rate of Fe(II) oxidation and precipitation from the pore water due to our simulated presence of ligands. When $f \to 0$, Fe(II) is effectively stable in the pore water for the maximum diffusive length scale we have assessed (0.47 cm/1.8 days). Calculated fluxes (J) are presented in Supplementary Table S1, where $f = 1$ and $f \to 0$. Refer to main article and Figure 9 for further details.

1

Supplementary Table S1. Parameterisation of diffusive Fe(II) flux calculations (Equations S1 to S5)

Site	I	T		pH	$[OH^-]$	$[O_2]_{BW}$	k	L	C_p		k_1	f	D_s	φ	J	
		(°C)	(°K)			mol L^{-1}	min^{-1}	cm	µmol L^{-1}	g cm^{-3}	s^{-1}		cm^2 s^{-1}		µmol m^{-2} d^{-1}	J_{norm}
Late Spring																
DY30_A	0.723	8.9	282	7.25	$1.78x10^{-7}$	$2.5x10^{-4}$	$2.42x10^{14}$	0.39	6.1	$5.03x10^{-7}$	$3.2x10^{-5}$	1	$2.98x10^{-6}$	0.77	23.9	1
DY30_A	0.723	8.9	282	7.25	$1.78x10^{-7}$	$2.5x10^{-4}$	$2.42x10^{14}$	0.39	6.1	$5.03x10^{-7}$	$3.2x10^{-5}$	→0	$2.98x10^{-6}$	0.77	30.0	1.3
Late Summer																
DY34_A	0.723	9.4	282.5	6.88	$7.59x10^{-8}$	$2.7x10^{-4}$	$2.47x10^{14}$	0.47	0.9	$5.03x10^{-8}$	$6.3x10^{-6}$	1	$3.03x10^{-6}$	0.77	3.6	1
DY34_A	0.723	9.4	282.5	6.88	$7.59x10^{-8}$	$2.7x10^{-4}$	$2.47x10^{14}$	0.47	0.9	$5.03x10^{-8}$	$6.3x10^{-6}$	→0	$3.03x10^{-6}$	0.77	3.9	1.08

L is equal to the mean oxygen penetration depth plus a diffusive boundary layer thickness of 0.06 cm.

C_p is the mean value (DY30 *n* = 11, DY34 *n* = 8) of [dFe(II)] beneath ***L***.

Where ***f***→0, an arbitrarily low value of 10^{-8} was used in calculations.

J is presented in alternative units to those derived by Equation S1.

2

Data repository (see accompanying data files)

Table S2: Concentrations of Fe and Mn in leachable sediment phases (displayed in Figure 3), and total carbon (total C), particulate organic carbon (POC) and particulate organic nitrogen (PON) contents (displayed in Figure S1) in shelf sediments in the Celtic Sea at Site A during late spring and late summer.

Table S3: Parameters in porewaters sampled from shelf sediments in the Celtic Sea at Site A during late spring and late summer, presented in Figure 3.

Table S4: Parameters in Core Top Water (bottom water collected on top of sediment cores) and bottom water collected with the titanium rosette in the Celtic Sea at Site A during late spring and late summer, presented in Figure 3.

Table S5: Water column dFe(II), sFe and dFe at site A in the Celtic Sea in July 2015 (Cruise DY033), presented in Figure 6. Water depth was 106 m.

References

Birchill AJ, Lohan MC, Milne A, Ussher SJ, Worsfold PJ, Hopkins J, Sharples J et al. (in prep) Iron deplete waters in the Celtic Sea following seasonal stratification. Geophysical Research Letters

Bowie AR, Achterberg EP, Sedwick PN, Ussher S, Worsfold PJ (2002) Real-Time Monitoring of Picomolar Concentrations of Iron(II) in Marine Waters Using Automated Flow Injection-Chemiluminescence Instrumentation. Environmental Science & Technology 36:4600-4607 doi:10.1021/es020045v

Conway TM, Rosenberg AD, Adkins JF, John SG (2013) A new method for precise determination of iron, zinc and cadmium stable isotope ratios in seawater by double-spike mass spectrometry. Anal Chim Acta 793:44-52 doi:http://dx.doi.org/10.1016/j.aca.2013.07.025

Homoky WB, John SG, Conway TM, Mills RA (2013) Distinct iron isotopic signatures and supply from marine sediment dissolution. Nat Commun 4 doi:10.1038/ncomms3143

29 Homoky WB, Severmann S, McManus J, Berelson WM, Riedel TE, Statham PJ, Mills RA
30 (2012) Dissolved oxygen and suspended particles regulate the benthic flux of iron
31 from continental margins. Mar Chem 134:59-70 doi:10.1016/j.marchem.2012.03.003

32 Hydes D, Aoyama M, Aminot A, Bakker K, Becker S, Coverly S, Daniel A et al. (2010)
33 Determination of dissolved nutrients (N, P, Si) in seawater with high precision and
34 inter-comparability using gas-segmented continuous flow analysers. In: The GO-SHIP
35 Repeat Hydrography Manual : A Collection of Expert Reports and guidelines. IOCCP
36 Report No 14, ICPO Publication Series No. 134, version 1, 2010. UNESCO/IOC,

37 Lacan F, Radic A, Labatut M, Jeandel C, Poitrasson F, Sarthou G, Pradoux C et al. (2010) High-
38 Precision Determination of the Isotopic Composition of Dissolved Iron in Iron
39 Depleted Seawater by Double Spike Multicollector-ICPMS. Anal Chem 82:7103-7111
40 doi:10.1021/ac1002504

41 Millero FJ, Sotolongo S, Izaguirre M (1987) The oxidation-kinetics of Fe(II) in seawater.
42 Geochim Cosmochim Acta 51:793-801

43 Nemzer BV, Dickson AG (2005) The stability and reproducibility of Tris buffers in synthetic
44 seawater. Mar Chem 96:237-242
45 doi:http://dx.doi.org/10.1016/j.marchem.2005.01.004

46 Nieuwenhuize J, Maas YEM, Middelburg JJ (1994) Rapid analysis of organic carbon and
47 nitrogen in particulate materials. Mar Chem 45:217-224
48 doi:http://dx.doi.org/10.1016/0304-4203(94)90005-1

49 Phillips RE, Ellis JH (1970) A rapid method of measurement of diffusion coefficients in
50 aqueous solutions. Soil Science 110:421–425

51 Raiswell R, Anderson TF (2005) Reactive iron enrichment in sediments deposited beneath
52 euxinic bottom waters: constraints on supply by shelf recycling. In: McDonald I,
53 Boyce AJ, Butler IB, Herrington RJ, Polya DA (eds) Mineral Deposits and Earth
54 Evolution, vol 248. Geological Society Special Publication. pp 179-194.
55 doi:10.1144/gsl.sp.2005.248.01.10

Scally S, Davison W, Zhang H (2006) Diffusion coefficients of metals and metal complexes in hydrogels used in diffusive gradients in thin films. Anal Chim Acta 558:222-229 doi:10.1016/j.aca.2005.11.020

Silburn B, Kröger S, Parker R, Sivyer D, Hicks N, Powell C, Johnson M et al. (submitted) Benthic pH gradients in a range of shelf sea sediments linked to sediments characteristics and seasonal variability. Biogeochemistry

Stookey LL (1970) Ferrozine - a new spectrophotometric reagent for iron. Anal Chem 42:779-& doi:10.1021/ac60289a016

Ussher SJ, Worsfold PJ, Achterberg EP, Laës A, Blain S, Laan P, de Baar HJW (2007) Distribution and redox speciation of dissolved iron on the European continental margin. Limnol Oceanogr 52:2530-2539

Waterbury RD, Yao W, Byrne RH (1997) Long pathlength absorbance spectroscopy: trace analysis of Fe(II) using a 4.5 m liquid core waveguide. Anal Chim Acta 357:99-102 doi:http://dx.doi.org/10.1016/S0003-2670(97)00530-8

Viollier E, Inglett PW, Hunter K, Roychoudhury AN, Van Capellen P (2000) The ferrozine method revisited: Fe(II)/Fe(III) determination in natural waters. Applied Geochemistry 15:785-790

Wehrmann LM, Formolo MJ, Owens JD, Raiswell R, Ferdelman TG, Riedinger N, Lyons TW (2014) Iron and manganese speciation and cycling in glacially influenced high-latitude fjord sediments (West Spitsbergen, Svalbard): Evidence for a benthic recycling-transport mechanism. Geochim Cosmochim Acta 141:628-655 doi:10.1016/j.gca.2014.06.007

Table S2

Click here to view linked References

Click here to download Attachment to Manuscript Table S2.xls.xlsx

Table S2: Concentrations of Fe and Mn in leachable sediment phases (particulate organic carbon (POC) and particulate organic nitr shelf sediments in the Celtic Sea at Site A during late spring

Depth	Fe_{asc}	$Fe_{H\text{-}HCl}$	Mn_{asc}	$Mn_{H\text{-}HCl}$	Total C
cm	µg/g	µg/g	µg/g	µg/g	% w/w
Late spring (cruise DY030)					
0-0.5	521	351	35.4	111	5.5
	513	321	36.5	107	
	498	340	34.9	111	
0.5-1	406	402	29.0	115	5.7
1-1.5	368		19.1		5.6
1.5-2	255		10.8		5.5
2-3	120		6.54		5.6
3-4	356		12.1		5.5
4-5	405		11.3		5.7
5-6	397		11.6		5.8
6-8	392		11.0		5.6
8-10	321		7.99		5.4
10-12	317		7.99		5.5
12-14	190		4.81		5.5
Late summer (cruise DY034)					
0-0.5	398	283	33.6	116	5.6
	243	300	24.6	117	
	274	301	27.2	109	
0.5-1	457	393	25.2	99	5.6
1-1.5	397		12.5		5.5
1.5-2	208		5.79		5.6
2-3	208		5.56		5.6
3-4	271		5.56		5.4
4-5	158		4.28		5.7
5-6	122		4.26		5.6
6-8	213		5.77		5.6
8-10	270		6.93		5.5
10-12	169		6.38		5.5
12-14	152		6.53		

displayed in Figure 3), and total carbon (total C),
ogen (PON) contents (displayed in Figure S1) in
and late summer.

POC	PON
% w/w	% w/w
1.29	0.143
1.46	0.157
1.34	0.139
1.21	0.136
1.13	0.136
1.22	0.141
1.37	0.146
1.42	0.160
1.28	0.146
1.04	0.120
0.98	0.104
0.98	0.108
1.23	0.139
1.33	0.138
1.22	0.136
1.21	0.132
1.13	0.124
1.09	0.121
1.10	0.127
1.04	0.125
1.01	0.116
1.08	0.118
1.08	0.122

Table S3

Click here to download Attachment to Manuscript Table S3.xls.xlsx

Click here to view linked References

Table S3: Parameters in porewaters sampled from shelf sediments in th

Depth	NO_3^-	NH_4^+	dMn	sMn	sFe(II)
cm	µmol L^{-1}	µmol L^{-1}	µmol L^{-1}	µmol L^{-1}	µmol L^{-1}
Late spring (cruise DY030)					
Core E, event 119					
0.5	1.96	31.6	33.5	32.6	13.0
1.5	0.92	46.4	35.8	34.7	42.5
2.5	0.57	68.0	29.5	28.5	111.6
3.5	0.11	76.9	26.7	25.7	147.6
5.5	0.23	101	23.2	22.3	166.1
7.5	0.09	117	20.7	19.9	123.8
9.5	0.28	122	16.9	16.4	91.4
11.5	0.24	130	15.1	14.6	78.4
Core H, event 119					
0.5	2.08	16.3	22.2	-	4.18
1.5	-	-	24.2	-	58.8
2.5	-	-	18.7	-	102
3.5	0.79	54.4	24.5	-	55.3
5.5	-	-	19.0	-	109
7.5	0.52	90.3	18.9	-	130
9.5	0.95	115	22.9	-	130
11.5	0.55	134	23.8	-	113
Core C, event 119					
0.5	1.25	9.4	26.9	-	7.29
1.5	0.71	30.2	32.2	-	0.385
2.5	0.49	24.0	24.4	-	16.9
3.5	0.72	29.3	33.0	-	19.0
5.5	0.58	23.6	9.1	-	32.6
7.5	0.69	45.4	25.3	-	64.6
9.5	-	-	19.4	-	129
11.5	0.15	127	19.0	-	138
Late summer (cruise DY034)					
Core F, event 71					
0.5	6.90	14.6	10.6	-	-
1.7	2.42	19.4	32.0	-	-
2.5	1.85	33.3	12.0	-	-
3.7	1.34	42.1	10.8	-	-
5.7	0.85	51.0	7.5	-	-
7.7	0.96	58.1	8.2	-	-
9.7	1.43	68.9	9.6	-	-
11.7	0.91	93.8	12.8	-	-
Core A, event 71					
0.5	2.87	20.2	39.8	-	-
1.5	1.30	32.0	43.3	-	-
2.5	0.35	53.9	23.9	-	-
3.5	0.79	53.1	26.6	-	-
5.5	0.78	63.6	26.1	-	-
7.5	0.91	74.4	25.4	-	-
9.5	1.15	73.6	13.3	-	-
11.5	2.68	80.4	11.7	-	-
Core G, event 71					
0.45	2.52	10.7	14.3	-	-

1.45	3.32	17.4	23.3	-	-
2.45	1.23	30.0	10.1	-	-
3.45	1.03	37.6	8.1	-	-
5.45	1.47	37.5	6.2	-	-
7.45	0.38	48.4	7.0	-	-
9.45	0.92	62.9	9.0	-	-
11.45	0.33	71.3	9.5	-	-

ıe Celtic Sea at site A during late spring and late summer, presented in Figure 3.

sFe μmol L^{-1}	**dFe(II)** μmol L^{-1}	**dFe** μmol L^{-1}	**δ^{56}dFe** ‰	**2 SD** ‰
14.7	13.4	14.8	-2.45	0.04
46.9	43.5	48.1	-2.93	0.04
123	113	124	-1.79	0.05
147	152	151	-1.55	0.05
162	170	169	-1.37	0.05
122	123	126	-0.92	0.05
88.6	93.2	93.0	-0.61	0.04
76.7	83.1	82.9	-0.80	0.04
4.54	4.56	5.35	-	-
65.1	60.1	66.2	-	-
112	102	115	-	-
53.8	56.2	54.8	-	-
107	112	113	-	-
130	133	134	-	-
128	134	134	-	-
117	118	115	-	-
8.10	7.59	8.44	-	-
0.405	0.411	0.433	-	-
18.5	18.5	20.5	-	-
19.3	19.8	19.8	-	-
32.8	35.0	33.5	-	-
64.7	66.4	65.8	-	-
128	132	131	-	-
137	140	138	-	-
-	0.337	0.358	-3.05	0.04
-	55.8	62.8	-2.29	0.04
-	76.3	84.3	-1.83	0.04
-	88.5	90.5	-1.68	0.04
-	97.1	98.7	-1.04	0.04
-	91.0	91.6	-1.01	0.04
-	87.8	89.1	-0.90	0.04
-	81.4	81.1	-0.74	0.04
-	1.17	1.19	-	-
-	9.5	10.9	-	-
-	100	112	-	-
-	77.9	76.9	-	-
-	107	109	-	-
-	118	119	-	-
-	108	108	-	-
-	60.4	60.5	-	-
-	1.23	1.34	-	-

-	15.1	17.6	-	-
-	70.0	76.8	-	-
-	115	116	-	-
-	88.1	90.6	-	-
-	67.0	67.8	-	-
-	93.1	94.2	-	-
-	87.7	90.1	-	-

Table S4

Click here to download Attachment to Manuscript Table S4.xls.xlsx

Click here to view linked References

Table S4: Parameters in Core Top Water (bottom water collected on top of sedim and bottom water collected with the titanium rosette in the Celtic Sea a

	Event	NO_3^-	NH_4^+	dFe(II)	dFe	δ^{56}dFe	2 SD
		µmol L^{-1}	µmol L^{-2}	nmol L^{-3}	nmol L^{-4}	‰	‰
Late spring (cruise DY030)							
BW, 12 m asf	84	8.00	0.30		5.44[b]	-0.22	0.04
CTW, Core E	119	-	-	-	18.27[b]	-1.02	0.04
CTW, Core H	119	7.96	1.19	14.6[a]	19.9[a]	-	-
CTW, Core C	119	8.47	0.99	14.2[a]	21.5[a]	-	-
Late summer (cruise DY034)							
BW, 4 m asf	3	8.41	0.39		10.07[b]	-0.26	0.04
CTW, Core F	71	8.20	1.06	-	13.79[b]	-0.11	0.04
CTW, Core A	71	7.87	0.44	-	-	-	-
CTW, Core G	71	8.08	0.38	-	-	-	-

dFe measurements in bottom waters made by isotope dilution during isotopic measurement

BW = bottom water

CTW = core top water

asf = above seafloor

[a]measurements from separate cores (ferrozine technique)

[b]concentrations determined by isotope dilution on MC-ICPMS

ıent cores)
ıt Site A, presented in Figure 3.

Table S5

Click here to download Attachment to Manuscript Table S5.xls.xlsx

Click here to view linked References

Table S5: Water column dFe(II), sFe and dFe at site A in the C presented in Figure 6. Water depth was 106 m.

Depth	**dFe(II)**	**SD**	**dFe**	**sFe**
m	pmol L^{-1}	pmol L^{-1}	nmol L^{-1}	nmol L^{-1}
21	<15	-	1.12	0.26
31	<15	-	0.41	0.18
51	71	32	4.13	1.02
81	-	-	2.94	0.96
93	231	3	5.62	-
98	280	20	6.50	1.20

eltic Sea in July 2015 (cruise DY033),